Homologous recombination between tandem paralogues drives evolution of Type VII secretion system immunity genes in firmicute bacteria

Stephen R. Garrett[1]*, Giuseppina Mariano[1], and Tracy Palmer[1]*

[1] Microbes in Health and Disease Theme, Newcastle University Biosciences Institute, Newcastle University, Newcastle upon Tyne, NE2 4HH, UK;

*To whom correspondence should be addressed.

e-mail: s.garrett2@newcastle.ac.uk, tracy.palmer@newcastle.ac.uk

Tel +44 191 208 3219

Running title: Expansion of T7 immunity gene families in firmicutes

ABSTRACT

The Type VII secretion system (T7SS) is found in many Gram-positive firmicutes and secretes protein toxins that mediate bacterial antagonism. Two T7SS toxins have been identified in *Staphylococcus aureus*, EsaD a nuclease toxin that is counteracted by the EsaG immunity protein, and TspA, which has membrane depolarising activity and is neutralised by TsaI. Both toxins are polymorphic, and strings of non-identical *esaG* and *tsaI* immunity genes are encoded in all *S. aureus* strains. During genome sequence analysis of closely related *S. aureus* strains we noted that there had been a deletion of six consecutive *esaG* copies in one lineage. To investigate this further, we analysed the sequences of the tandem *esaG* genes and their encoded proteins. We identified three blocks of high sequence homology shared by all *esaG* genes, and identified evidence of extensive recombination events between *esaG* paralogues facilitated through these conserved sequence blocks. Recombination between these blocks accounts for loss of *esaG* genes from *S. aureus* genomes. TipC, an immunity protein for the TelC lipid II phosphatase toxin secreted by the streptococcal T7SS, is also encoded by multiple gene paralogues. Two blocks of high sequence homology locate to the 5' and 3' end of *tipC* genes, and we found strong evidence for recombination between *tipC* paralogues encoded by *Streptococcus mitis* BCC08. By contrast, we found only a single block of homology across *tsaI* genes, and little evidence for intergenic recombination within this gene family. We conclude that homologous recombination is one of the drivers for the evolution of T7SS immunity gene clusters.

Key Words: T7SS, homologous recombination, immunity gene families, *Staphylococcus aureus, Streptococcus*

INTRODUCTION

The type VII protein secretion system (T7SS) is found in many Gram-positive bacteria. Following its discovery in pathogenic Mycobacteria, it has since been described in a range of other actinobacteria and in firmicutes (1-5). Cryo-electron microscopy studies have shown that the ESX-5 T7SS from Mycobacteria exists as a 2.3 mDa membrane complex, with a central ATPase, EccC, forming a hexameric pore (6, 7). The firmicutes T7SS is only distantly related to the actinobacterial T7SSa system, and has been designated T7SSb. The hexameric ATPase is the only common component found across all T7SSs, and is designated EssC in the T7SSb systems (8, 9).

While the T7SSa is heavily linked with Mycobacterial virulence, there is growing evidence that the T7SSb plays an important role in bacterial antagonism (10, 11). In *Streptococcus intermedius*, three T7SSb-secreted antibacterial effectors have been identified, including TelB, an NADase, and TelC a lipid II phosphatase (12). The *Enterococcus faecalis* T7SSb also mediates contact-dependent inhibition of some firmicute bacteria, and a bioinformatic analysis in *Listeria monocytogenes* has identified over 40 potential antibacterial substrates of the T7SS (13, 14).

A role for the T7SSb in interbacterial competition was first characterised in the opportunistic pathogen *Staphylococcus aureus* (15). The T7SS-encoding locus in this organism is highly variable. Sequence divergence initiates towards the 3' end of *essC*, with *essC* sequences falling into one of four variants, termed *ess1* – *ess4* (16). Downstream of each *essC* subtype is a cluster of variant-specific genes. In *essC1* variant strains one of these genes, *esaD*, encodes a secreted nuclease toxin with antibacterial activity. Protection from the toxic activity of EsaD is mediated by EsaG, which is encoded immediately adjacent to *esaD* in *essC1* strains. EsaG inactivates EsaD by forming a tight complex with the EsaD nuclease domain (15). While all *essC1* strains encode *esaD*, the toxin nuclease domain is polymorphic, and these strains also encode additional copies of *esaG* genes in a highly variable immunity gene

66 island located at the 3' end of the *ess*/*T7SS* locus (10, 15, 16). These additional *esaG* copies
67 are genetically diverse, but share some core regions of similarity within the encoded amino
68 acid sequences (17, 18). Strings of up to nine non-identical *esaG* genes are also found in a
69 similar genomic location in *essC2*, *essC3* and *essC4* strains (10).
70
71 TspA is a second antibacterial toxin secreted by the *S. aureus* T7SS. TspA has a C-terminal
72 membrane-depolarising domain, and immunity from intoxication is provided by the membrane-
73 bound TsaI protein (19). The *tspA-tsaI* locus is encoded distantly from the T7 gene cluster,
74 and is found across all four *essC* variant strains. Similar to EsaD, the TspA toxin domain is
75 polymorphic, and all strains encode clusters of TsaI variants (between two and sixteen copies)
76 directly downstream of *tspA* (19).
77
78 It is common for bacteria to encode repertoires of immunity proteins for protection against
79 polymorphic effector proteins. For example, bacteria in the gut accumulate immunity genes in
80 genomic islands that provide protection against type VI secretion system effectors (20). This
81 includes orphan immunity genes in strains that do not encode the cognate effector protein, as
82 we observe for *esaG* genes in *S. aureus essC2*, *essC3* and *essC4* strains that do not contain
83 *esaD*. While it is common for immunity islands to carry many predicted immunity genes, it is
84 less common to see so many homologues of the same immunity gene clustered together. At
85 present, little is known about the origin of the T7SS immunity repertoires.
86
87 The *Staphylococcus aureus* strain NCTC8325, and its derivatives, are commonly used as a
88 model strains for laboratory studies (21). NCTC8325 was initially isolated from a corneal ulcer
89 and has been used extensively for the propagation of the lysogenic bacteriophage
90 *Staphylococcus* virus 11 (Previously Phage 47) (22). Since NCTC8325 also carries two other
91 lysogens in its genome, *Staphylococcus* viruses 12 and 13 (23) UV-induced curing was used
92 to rid the strain of prophage, to give strain RN450 (24) (Fig 1a). RN450 has been used to

construct many laboratory strains over the years, including RN6390, which is one of the key strains we have employed for T7SS secretion studies (e.g. (25, 26)).

During our analysis, we found that there were two separate genome sequences reported for NCTC8325. When comparing the first sequence, published in 2006 (GenBank accession number CP000253; (27)), with the later sequence (uploaded in 2018 by the Wellcome Trust Sanger Institute to GenBank; accession number LS483365) we noted that there were a number of differences, including in *esaG* repertoire encoded at the 3' end of the *ess* gene cluster (Fig 1b). In this study we used whole genome sequence analysis to identify which of these two genome sequences was most closely related to RN6390. We subsequently used gene phylogeny and cluster analyses to identify the processes that drive the accumulation of T7SS immunity genes. Our findings indicate that intergenic recombination is a major factor in the evolution of *esaG* genes. We also noted that a similar process drives the evolution of *tipC* genes, which encode Streptococcal TelC immunity proteins (12). By contrast, while there is some evidence of intergenic recombination within *tsaI* clusters, it does not appear to be the main mechanism of evolution for this gene family.

METHODS

Strains, genome sequencing and phylogenic analysis of prophage

Strain RN6390 was obtained from Professor Jan Maarten van Dijl (University of Groningen, NL). All other strains were obtained from Professor José Penadés (Imperial College, UK). All genome sequencing was carried out by MicrobesNG (Birmingham, UK) with enhanced genome sequencing for RN6390 and standard whole genome service for RN25 and RN450; sequences are available at NCBI under accession numbers CP090001.1, JAJSOX000000000.1 and JAJSOY000000000.1, respectively. Whole genome alignment was executed using progressiveMauve (28). SNP calling was carried out using Snippy v4.6.0 (29). To determine the taxonomy of the phage identified in RN6390 strain, its nucleotide sequence was submitted to VIPTree browser with default parameters (30). From the resulting proteomic tree, phage genomes associated with *S. aureus* species were selected to generate the tree in Fig 2.

Gene and protein alignment

Nucleotide sequences were obtained from NCBI and aligned with MAFFT v7.489 (31). Amino acid sequences were obtained from NCBI and aligned using MUSCLE v3.8.1551 (32). To construct similarity plots for both nucleotide and amino acid sequences, Plotcon (https://www.bioinformatics.nl/cgi-bin/emboss/plotcon) was executed using aligned sequences, with a window size of 5. For *esaG4,* the full pseudogene was used for the nucleotide alignment. For the alignment of the EsaG4 amino acid sequence, the two predicted open reading frames (ORFs) were used. For Plotcon analysis on large input sequences, alignments were manually curated to remove partial sequences and pseudogenes.

Recombination Prediction

Aligned nucleotide sequences were opened in the RDP4 software (33) and Run All selected. TrimAl v1.2 (34) was used to remove the unaligned 5' region of *tsaI* genes before RDP4 analysis was carried out.

Gene phylogeny

Maximum likelihood trees for nucleotide sequences were built with IQTREE v 2.1.4 (35), with 1000 ultrafast bootstraps. Trees were visualised and annotated using iTOL (36).

Comparison of genetic loci and gene cluster analysis

T7SS-encoding loci from each variant were subjected to pairwise comparisons with the RN6390 *T7SS* locus using BLAST (37). A similar approach was used to compare *Staphylococcus* phage RN6390 with *Staphylococcus* phage SAP40 genomes. The report produced by BLAST was used as a comparison file in genoPlotR package (38) within RStudio (39) to plot regions of similarities between the two loci. FlaGs (40) was used to assess the variation in number of *tsaI* repeats across *S. aureus* strains. Examples were selected to represent diversity at this locus.

Construction and analysis of a plasmid database

A database containing all available plasmid sequences was built from PLSDB (https://ccb-microbe.cs.uni-saarland.de/plsdb/plasmids/) (41). Subsequently, Hmmsearch from the HMMER suite (v 3.3.2) (42) was used to identify *esaG* or *tsaI* genes encoded within the database. For each *esaG* or *tsaI* copy identified, efetch from the entrez-utilities (43) was used to retrieve the specific assembly ID where the genes were encoded. EsaG and TsaI proteins identified as encoded on plasmids together with their corresponding assembly ID, were then analysed using FlaGs to define the specific gene neighbourhood of *esaG* and *tsaI* on these assemblies.

RESULTS

Analysis of the RN6390 genome.

Two genome sequences are available for NCTC8325, here designated NCTC8325-Oklahoma (GenBank accession number CP000253) and NCTC8325-Sanger (GenBank accession number LS483365). The genomes of NCTC8325-Oklahoma and NCTC8325-Sanger were aligned to identify differences between the strains (Table S1). Following SNP calling and manual curation we identified a total of 78 SNPs and other small polymorphisms between these two strains. We also identified a duplication of 16S and 23S ribosomal RNA genes in NCTC8325-Oklahoma relative to NCTC8325-Sanger (Table S1). A further notable difference is that NCTC8325-Sanger carries six additional *esaG* genes, relative to NCTC8325-Oklahoma, at the *ess* cluster (Table S1, Fig 1b).

In order to identify which NCTC8325 strain is the likely precursor strain of RN6390, we carried out whole genome sequencing of RN6390 (GenBank accession number CP090001.1) and aligned it with the genomes of NCTC8325-Oklahoma and NCTC8325-Sanger, respectively. Differences between RN6390 and each NCTC8325 strain are recorded in SNP tables (Tables S2 and S3). As expected, a major difference found between both NCTC8325 genomes and RN6390 is the presence of three prophages in the NCTC8325 genomes which were successively cured out during the construction of the RN6390 progenitor, RN450 (Fig 1a). A prophage, *Staphylococcus* phage 6390 (φ6390) has been identified previously in the genome of RN6390, integrated in the *rpmF* gene (44, 45). This is at a different locus from the three prophage loci found in the two NCTC8325 genome sequences. To determine whether φ6390 is related to any of the prophages cured from NCTC8325, the genome sequence was extracted and used to determine its taxonomy. As shown in Fig 2, φ6390 is a distinct prophage to those cured from NCTC8325. Analysis of φ6390 using blastn gave an almost identical match to *Staphylococcus* phage SAP40 (GenBank accession number: MK801683.1, 99%

188 coverage and 99.98% identity). As φ6390 is not present in RN4220, this suggests that it was
189 introduced during genetic manipulation steps performed following generation of RN450.
190
191 Further analysis of the RN6390 genome sequence revealed that it aligned more closely to
192 NCTC8325-Sanger than NCTC8325-Oklahoma, and also carries the six additional *esaG*
193 genes found in NCTC8325-Sanger. This suggests that NCTC8325-Sanger is the likely
194 progenitor of the 8325 lineage. To confirm this, we sequenced the genomes of the
195 intermediate strains RN25 and RN450 (Genbank accession numbers JAJSOX000000000.1
196 and JAJSOY000000000.1, respectively), as they are directly on the lineage of RN6390. Both
197 of these strains share the additional copies of *esaG* and other genomic features of NCTC8325-
198 Sanger, confirming that this strain is likely to be the true parent of RN6390.
199
200 The origin of the NCTC8325-Oklahoma strain from GenBank accession CP000253 is
201 described as the 'University of Oklahoma Health Sciences Center'. This strain is clearly closely
202 related to NCTC8325-Sanger, but may potentially have accumulated mutations through serial
203 passaging within a laboratory setting. Strikingly, the biggest difference between the two strains
204 apart from the ribosomal RNA gene duplication is the loss of the six *esaG* homologues.
205
206 **Intergenic recombination is a driving force in the evolution of *esaG* genes.**
207 To determine how the six *esaG* copies may have been lost in NCTC8325-Oklahoma, we
208 examined this region of the chromosome in more detail. RN6390 encodes 12 homologues of
209 *esaG*, all of them at the *ess* gene cluster. The first copy is found directly downstream of *esaD*
210 and encodes the cognate immunity protein for the nuclease toxin (Fig 3a)(15). We have named
211 this *esaG1*. This is followed by three genes encoding hypothetical proteins (SAOUHSC_00270
212 _00271 and _00272), before a stretch of four further *esaG* homologues (*esaG2* - *esaG5*). This
213 is followed by a further homologue of *SAOUHSC_00270* (annotated as *SAOUHSC_00270b*
214 on Fig 3a, sharing 96.49% identity with *SAOUHSC_00270*) and then an additional seven *esaG*
215 homologues (*esaG6* – *esaG12*; Fig 3a). Note that while *esaG4* is annotated as a pseudogene,

due to a short additional stretch of nucleotides close to the centre of the gene introducing a premature stop and subsequent start codon, it actually encodes two smaller ORFs (Fig 3a). A genome alignment using progressiveMauve predicts that the genomic deletion in NCTC8325-Oklahoma spans *esaG2 – esaG7.*

To assess variation between the 12 homologues of EsaG, the amino acid sequences were aligned (Fig 3b), and regions of homology between the proteins were analysed using Plotcon (Fig 4a). Numerous regions of sequence homology were observed, including two major blocks of high sequence homology at amino acids 13-31 and 84-119. To assess whether these were general features of *S. aureus* EsaG proteins, we downloaded approximately 4,000 *S. aureus* EsaG sequences from RefSeq and collectively analysed them using Plotcon. Fig S1a indicates that a similar profile of homology is seen across all EsaG proteins.

We next examined the intergenic regions between the RN6390 *esaG* homologues. Strikingly, we noted that most of the intergenic regions were of a very similar length, other than when they directly preceded a non-*esaG* gene (for example *SAOUHSC_00270b*). They also share a high degree of homology (Fig S2a). When we undertook Plotcon analysis on the *esaG* genes, including the 3' intergenic regions (Fig 2a, Fig S2b), we noted the same two major blocks of homology that we had seen from the amino acid analysis, but in addition a third block encompassing the end of the gene and the downstream intergenic region (Fig 3a, Fig S2b, Fig S3).

Given the substantial levels of homology between the *esaG* genes, we used the recombination prediction software, RDP4, to determine whether there had been recombination events between the genes. The RDP4 output, shown in Table S4 and summarised Fig 4b, predicts with high significance that there have been extensive recombination events within most (but not all) of these genes. As shown in Fig 4b, recombination appears to occur at the three points within the genes that correspond to the regions of high nucleotide sequence homology (Fig

4b, Table S4). To support these findings, we constructed a maximum-likelihood tree for the 12 *esaG* genes (Fig 4c). No recombination is predicted within *esaG3*, which is genetically distant from other *esaG* homologues. Conversely, *esaG2* and *esaG5* appear to vary only in their central regions, and these cluster closely on the tree (Fig 4c), consistent with the RDP4 output.

Based on the RDP4 results, we built a schematic representation showing the homologous regions of the *esaG* genes that are likely involved in the recombination events (Fig 4d). Specific regions of the genes seem to share high homology with others, for example, the mid-section of many of the homologues share high homology to equivalent sections of *esaG1* (coloured teal). Conversely, genes such as *esaG3* and *esaG6* appear to be much more diverse. Based on our observations, it is probable that a recombination event between the first conserved regions of *esaG2* and *esaG8* was responsible for the loss of the seven genes at this locus in NCTC8325-Oklahoma. This is corroborated by an alignment of the nucleotide sequences of *esaG2* and *esaG8 with SAOUHSC_00274* (Fig S2c). The alignment indicates that *SAOUHSC_00274* is mosaic comprising the 5' region of *esaG2* with the middle and 3' sections of *esaG8*, consistent with recombination at homology block 1 (Fig S2d).

esaG recombination in an epidemic strain of _S. aureus_

USA300 is a methicillin-resistant *S. aureus essC1* strain, and a dominant cause of community-acquired *S. aureus* infection in the USA (46). A recent study analysed the community spread and evolution of a USA300 variant during a New York outbreak (47). Comparing the whole-genome sequences of the epidemic lineage showed that these strains carry only seven *esaG* genes in comparison to the ten copies in the closely related USA300 FPR3757. Using strain BKV_2 as a representative of the outbreak lineage, we aligned the region spanning from *esaE* to *SAUSA300_0303* with USA300 FPR3757. The alignment showed almost complete sequence identity, other than in a region spanning from the middle of *SAUSA300_0295* to the middle of *SAUSA300_0299* (Fig S4a) which was absent from BKV_2. When the nucleotide

sequences of *SAUSA300_0295* and *SAUSA300_0299* were aligned with *esaG4* of BKV_2, *esaG4* was again seen to be mosaic, with most of the gene being identical to *SAUSA300_0295* but the 3' end showing 100% identity to *SAUSA300_0299* (Fig S4b). This is consistent with recombination between homology block 2 of *SAUSA300_0295* and *SAUSA300_0299*, with loss of the intervening DNA.

esaG diversity across _S. aureus essC2_, _essC3_ and _essC4_ variants.

Although *S. aureus essC2*, *essC3* and *essC4* variants do not encode EsaD, these strains all accumulate *esaG* genes at the 3' end of their T7SS-encoding loci. To ascertain whether the homologues of *esaG* encoded in these strains are close relatives of those found in RN6390, we analysed the *esaG* genes encoded in strains ST398, MRSA252 and HO 5096 0412, as representatives of *essC2*, *essC3* and *essC4* variants, respectively. The sequence of the *T7SS* loci for each of these strains was subjected to pairwise comparison, using BLAST, with the RN6390 locus, and further analysed using genoPlotR (48) to produce a graphic representation of the alignment of these regions (Fig 5). In this output, regions of homology are highlighted by red-connecting blocks, and the colour intensity of these blocks reflects the percentage identity found between the two compared regions.

As shown in Fig 5a, the *essC2* strain, ST398, shares higher homology with the RN6390 *T7SS* cluster than either MRSA252 or HO 5096 0412. This strain harbours two intact copies of *esaG* (*SAPIG_0310* and *_0311*), and one pseudogene (covering the two small genes *SAPIG_0314-0315*, and herein referred to as a single *SAPIG_0314* pseudogene). We used RDP4 analysis with *esaG1-12* from RN6390, and phylogenetic tree construction, to determine whether there were any regions of shared homology. The analysis showed that *SAPIG_0314-0315* has the highest homology to *esaG12* (Fig 5a) and appears to cluster in the same branch of the phylogenetic tree (Fig 5d). No recombination events are predicted for this pseudogene, suggesting this is most likely a copy of *esaG12* that has accrued mutations (Fig S5a). Conversely, *SAPIG_0310* and *SAPIG_0311* have much lower homology to the *esaG*

300 homologues in RN6390 (Fig 5a), although recombination events are predicted with *esaG4* for
301 *SAPIG_0310* and with *SAPIG_0314-315* for *SAPIG_0311* (Fig S5a).
302
303 The *essC3* strain, MRSA252, has four tandem *esaG* homologues at its *ess* locus, *SAR_0293*
304 - *SAR_0296* (Fig 5b). These are predicted by BLAST to share the highest homology with
305 RN6390 *esaG9-esaG12*. However, these homologues do not cluster together in the
306 phylogenetic tree (Fig 5d), and for example *SAR_0295*, predicted by genoPlotR to be a
307 homologue of *esaG11*, clusters with *esaG3.* Recombination events are also detected for all of
308 the *esaG* genes in MRSA252 (Fig S5b).
309
310 The *essC4* strain, HO 5096 0412, harbours two *esaG* copies, *SAEMRSA15_02570* and
311 *SAEMRSA15_02580*, which are predicted by BLAST to share highest homology with *esaG11*
312 and *esaG12*, respectively (Fig 5c). However, phylogenetic analysis indicates that
313 *SAEMRSA15_02580* clusters with *esaG11* as opposed to *esaG12*, and *SAEMRSA15_02570*
314 does not cluster closely with any of the RN6390 *esaG* genes (Fig 5d). RDP4 analysis also
315 predicts recombination events for both genes in HO 5096 0412 (Fig S5c).
316
317 In summary, whilst *SAPIG_0314-0315* is a copy of *esaG12*, the remaining *esaG* homologues
318 found in the three representative strains of *essC* variants 2, 3 and 4 all appear to be
319 recombinants. Some of the recombination events are between homologues present in these
320 strains (Tables S5 - S7), suggestive of common ancestry. However, for other recombination
321 events, the parent *esaG* gene is unknown and is not present in any of these representative
322 strains.
323
324 **Accumulation of *tsaI* genes in the RN6390 genome.**
325 TspA is a T7SS-secreted antibacterial toxin that is highly conserved across all *essC* variant
326 strains (19). In all of these strains it is encoded away from the T7SS gene cluster, at a genomic
327 location bounded by *SAOUHSC_00583* and *iolS* (*SAOUHSC_00603*). The toxic activity of

328 TspA is neutralised by TsaI, a membrane protein of the DUF443 family (19). Multiple copies
329 of *tsaI* genes are encoded downstream of *tspA* (Fig 6, Fig S6), and in RN6390 there are 11
330 copies, *tsaI1* – *tsaI11* (Fig 6a). A small pseudogene, encoded by *SAOUHSC_00600* shares
331 homology to part of the toxin region of TspA and is also found at this locus.
332
333 We wondered whether recombination events, similar to those we have observed for *esaG*
334 genes, also contributed to the evolution of *tsaI* genes. An alignment of the amino acid
335 sequences for RN6390 TsaI proteins (Fig 6b), shows that there is much greater sequence
336 variability between these proteins than the EsaG homologues. This is particularly apparent in
337 the C-terminal region of the protein, with only limited sequence identity observed between TsaI
338 homologues. Similar variability was observed in a representative alignment of around 3000
339 TsaI sequences (Fig S1b). Much greater variability was also observed in the *tsaI* intergenic
340 regions, in both length and DNA sequence compared with *esaG* (Fig 6c).
341
342 To identify the regions of highest homology at both the protein and DNA level, we ran Plotcon
343 analysis of the 11 *tsaI* genes and their encoded ORFs. Unlike EsaG, TsaI homologues have
344 only a single region of high similarly, covering approximately the first 75 amino acids, which is
345 also mirrored at the DNA level (Fig 7a, Fig S7). As only one block of high homology is detected
346 and there is a high degree of sequence variability in the *tsaI* intergenic regions, recombination
347 within individual genes is unlikely. To analyse this, we used RDP4 to predict recombination
348 events within the 11 homologues of *tsaI* genes (Fig 7b). Far fewer potential recombination
349 events were predicted than for *esaD* genes, and with lower probability, which could arise from
350 evolutionary processes other than recombination (Table S8).
351
352 **_tsaI_ genes are found on Staphylococcal plasmids**
353 Horizontal gene transfer (HGT) is a major mechanism for the movement of genomic material
354 between bacteria (49). Plasmids are one of the key drivers of HGT and help to mediate the
355 spread of resistance genes among bacterial populations (e.g. 50, 51). To investigate whether

the *esaG* and/or *tsaI* toxin resistance genes may also be disseminated by plasmids, we constructed a database of bacterial plasmids as described in the methods section and interrogated this for the presence of *tsaI* and *esaG* genes. We identified a single Staphylococcal plasmid carrying an *esaG* gene and five Staphylococcal plasmids that encode one or more TsaI homologues (Fig 8). Two of the five plasmids encoding TsaI (pCAPBN21 and an unnamed plasmid from *Staphylococcus caprae* 26D) also encode a full-length TspA along with the two WXG100-like proteins (DUF5344 and DUF3958 family proteins) that have been proposed to serve as TspA-specific T7SS targeting factors (10). A further two plasmids (pSB1-57-a and an unnamed plasmid from *Staphylococcus warneri* SWO) code for a fragment of TspA alongside TsaI, with the SWO plasmid also encoding two further *tsaI* genes. An unnamed plasmid from *Staphylococcus simulans* MR1 encodes an orphan *tsaI* with no detectable *tspA* remnant. The SWO plasmid is particularly interesting as this carries further T7-related genes including the *esaG* we identified along with a portion of *esaD*, and a fragment of an HNH-nuclease gene along with a SM1/KNR4 protein encoding gene (a family implicated as a nuclease immunity protein (52) and found in Staphylococcal T7SS immunity gene islands (10)). For three of the plasmids, the immunity genes are close to recombinase genes, which may provide a mechanism for their accumulation, and four of them carry nearby *IS* elements that could facilitate their transfer to the chromosome without the need for homologous recombination.

Intergenic recombination between *tipC* immunity genes in *Streptococcus*.

Three T7SS-secreted antibacterial toxins have been identified in *Streptococcus intermedius*. TelA and TelB are both cytoplasmic-acting toxins neutralised by the TipA and TipB immunity proteins, respectively (12). Our genome analysis indicates that strains generally encode only a single *tipA* gene, while *tipB* is found in up to five copies. The third *S. intermedius* toxin is TelC, a lipid II phosphatase. Protection from TelC toxicity is provided by TipC, a membrane-bound immunity protein that faces the extracellular space (12, 53). Klein *et al*. reported that the number of *tipC* genes encoded at the *telC* locus was highly variable between strains (53).

We used gene neighbourhood analysis across Streptococcal genomes to compare the number of *tipC* genes present at the *telC* gene cluster, identifying 15 of them in a strain of *Streptococcus mitis* BCC08 (Fig 9a).

Alignment of the *S. mitis* BCC08 TipC sequences and their encoding DNA (Fig 9b, Fig S8) showed two regions of high sequence conservation close to the start and end, with a central region of much higher sequence variability (Fig 10a). Using RDP4 to screen for recombination, at least five recombination events were predicted between these genes (Fig 10b, Table S9), in each case almost certainly through the blocks of high homology we identified. To analyse this further we constructed a maximum likelihood tree to compare *tipC* homology. Genes *D8786_RS05910* and *D8786_RS0585* cluster closely in this tree, which corresponds to the recombination event predicted between these two genes (Fig 10b, Table S9). Likewise *D8786_RS05920*, which is predicted to be the major parent to *D8786_RS05865* (Table S9) also clusters phylogenetically with this gene. We conclude that similar to *esaG*, intergenic recombination drives the evolution of *tipC* immunity gene repertoires.

DISCUSSION

Through comparative genome analysis we noted that the *esaG* copy number is distinctly different in closely related strains of *S. aureus*, a finding that had also been previously described within the NCTC8235 lineage (17). To investigate how copy number variability may arise, we undertook sequence analysis of EsaG proteins and their encoding DNA, including their 3' flanking regions. We found three blocks of highly conserved nucleotide sequence, a large central one of approximately 100 nucleotides in length, and a 5' and 3' block both of around 55 nucleotides each. Homologous recombination occurs at regions of high homology within nucleotide sequences (Reviewed in 54). The minimum length requirement for efficient recombination in *S. aureus* is unclear, but stretches of 40-70 nucleotides have been reported for other bacteria (e.g. 55 - 57). Using RDP4 to predict recombination within *esaG* genes, we found strong evidence for recombination, corresponding to events within each of the three homology blocks we identified. Furthermore, our analysis revealed that the loss of six *esaG* genes in NCTC8325-Oklahoma arose from recombination across homology block 1, whereas three *esaG* genes have been lost in an outbreak strain of USA300 through recombination across homology block 2.

Previous work has reported that the *S. aureus* tandem-like lipoproteins, encoded on the νSaα island, also show extensive copy number variation across strains (58, 59). Similar analysis to that reported here showed that each *lpl* gene shares a stretch of approximately 130 nucleotides of high homology in its central region. Recombination was demonstrated to occur between the central conserved region of one gene and the same region of the neighbouring gene (57), thus spanning the 3' portion of gene 1, the intergenic region and the 5' region of gene 2.

To investigate whether intergenic recombination might represent a general mechanism for the evolution of T7SS immunity gene families, we examined the organisation of the *tipA*, *tipB* and *tipC* immunity genes in Streptococci. It has previously been noted that *tipC* copy number is

427 highly variable in Streptococcal genomes (53), and our analysis identified that up to 15 copies
428 of *tipC* could be present. Examination of recombination events within *tipC* revealed that
429 intergenic recombination is also a feature, and that it primarily occurs between homologous
430 blocks of sequence identity at the start and end of the genes. The structure of TipC reveals
431 that it has seven beta strands forming a concave face, with three alpha helices made up from
432 the N- and C-terminal regions of the protein (53, Fig 10d). Analysis of colicin DNase toxins
433 and their immunity proteins has shown that sequence divergence between related toxins and
434 immunities tends to concentrate at the binding interface (60). In agreement with this, site-
435 directed mutagenesis has strongly implicated the concave face as the region that binds to
436 TelC, and this region of TipC shows the highest level of sequence divergence (Fig 10d; 53).
437 We speculate that for EsaG the regions of high homology are not directly involved in toxin
438 binding, but may provide a structural framework on which amino acid substitutions in the
439 variable regions accumulate to alter the toxin binding specificity. Mechanisms to allow rapid
440 evolution of immunity proteins are likely to be essential to allow strains to rapidly acquire
441 resistance to novel toxin variants.
442
443 TspA is a second polymorphic toxin encoded by *S. aureus*. Protection from its membrane-
444 depolarising activity is provided by the immunity protein TsaI (19). TsaI is a polytopic
445 membrane protein predicted to have five transmembrane domains. As with *esaG*, multiple *tsaI*
446 genes are found in *S. aureus* genomes, however, our analysis has indicated that there is little
447 evidence of recombination between them. We found only a single block of high nucleotide
448 sequence homology at the 5' end of *tsaI* genes. This encodes approximately the first 75 amino
449 acids of TsaI, which would encompass the first two transmembrane domains. At present it is
450 not known whether TsaI neutralises TspA though direct interaction, or through the
451 sequestering of a membrane-bound partner protein with which TspA must interact to facilitate
452 its insertion or folding (or a combination of both of these). In this context, membrane
453 permeabilising peptide bacteriocins produced by some Gram-positive bacteria require a
454 membrane-bound receptor, such as the membrane components of the mannose

phosphotransferase system, for their activity. In the case of the *Lactococcus lactis* lactococcin A bacteriocin, the immunity protein LciA acts through formation a complex with both the receptor protein and the bacteriocin (61). By analogy it is possible that the first two transmembrane domains of TsaI interact with a candidate receptor, constraining their sequence, whereas the remainder of the immunity protein binds to the toxin and is therefore under diversifying selection. At present it is unclear how *tsaI* gene clusters evolve, although we did note that there was evidence for carriage of *tsaI* genes on Staphylococcal plasmids, which may facilitate gene movement within and between strains. Further work would be required to clarify the mechanisms that drive *tsaI* diversity.

ACKNOWLEDGEMENTS

We thank Prof Jan-Maarten van Dijl (University of Groningen, NL) for providing us with strain RN6390, and Prof José Penadés (Imperial College, UK) for providing all of the other strains in this study. We thank Prof Victor J. Torres and Dr Alejandro Pironti (NYU Langone, USA) for providing the genome sequence of USA300 BKV_2. This work was supported by Wellcome through Investigator Award 110183/A/15/Z to TP and Sir Henry Wellcome Postdoctoral Fellowship 218622/Z/19/Z to GM. SG is funded by the Newcastle-Liverpool-Durham BBSRC DTP2 Training Grant, project reference number BB/M011186/1.

FIGURE LEGENDS

Figure 1. Lineage of NCTC8325 daughter strains. a. A selection of daughter strains of the NCTC8325 lineage and how they were generated. RN25 (also called 8325-3) was generated from NCTC8325 following UV curing of prophages 11 and 12 (23). RN450 (also called 8325-4) was generated from RN25 by a second round of UV exposure, to cure prophage 13 (23). Methylnitronitrosoguanidine (MNNG)-mediated mutagenesis of RN450 was used to generate RN4220, which is restriction deficient and capable of accepting foreign DNA (62). RN450 was separately transduced with pRN3032, a Tn551 donor plasmid to generate RN1478 (63) ISP479 is a cadmium-resistant revertant of RN1478 (64). RN6390 was generated from ISP479 by curing of pRN3032 (24). b. The genetic layout of the *ess* locus in NCTC8325- Oklahoma and NCTC8325-Sanger. The dashed lines and bar represent the region that is missing from NCTC8325-Oklahoma, as identified in this study.

Figure 2. Analysis of *Staphylococcal* phage 6390. A phylogenetic tree of φ6390 against a database of *Staphylococcal* phages generated using VIPtree (29). The positions of φ6390 and *Staphylococcal* phages 11, 12 and 13 (excised from the NCTC8325 parent strain during construction of RN6390) on the tree are indicated with red stars.

Figure 3. Homologues of *esaG* encoded at the *ess* locus in RN6390. a. Illustration of the 3' of the RN6390 *ess* locus which encodes the T7SS nuclease toxin, EsaD, its cognate immunity protein, EsaG and 11 further homologues of EsaG (numbered *esaG2* – *esaG12*). Genes *esaG2* to *esaG7* are indicated by a black bar, and are absent from NCTC8325-Oklahoma, while the dotted line indicates the actual region lost by recombination. Note that *esaG4* is shown in hatched shading because it is annotated as a pseudogene. However, it does encode two predicted ORFs, EsaG4i and EsaG4ii. b. Sequence alignment of EsaG homologues encoded by RN6390. The black boxes represent regions of high homology based in this alignment.

Figure 4. Recombination within the RN6390 *esaG* homologues. a. Regions of high homology across the RN6390 EsaG protein sequences (middle panel) and the corresponding nucleotide sequences (bottom panel). The positions of blocks of high homology are shown in grey shading and along with their relative positions along the gene sequence (top panel). The basepair positions that define the conserved regions are taken from the nucleotide sequences of *esaG1*. b. RDP4 was used to predict recombination events within the *esaG* homologues encoded by RN6390. The identity of each gene is given in black at the left, with regions of recombination labelled directly below, in the colour of the gene from which the recombinant section originated. c. A maximum likelihood tree was generated for RN6390 *esaG* homologues in IQTREE and visualised and annotated in iTOL. d. Illustration of regions of homology in the *esaG* homologues in RN6390. Black bars represent conserved regions of the gene and the variable regions have been assigned a colour and corresponding number. Homologous regions are coloured with the same colour. Numbers were assigned based on the first gene in the series that had the unique variable region. White hatched shading indicate a pseudogene.

Figure 5. Recombination events within the *esaG* genes encoded in representative *essC2*, *essC3* and *essC4* variant strains. a-c. The genes downstream of *essC* are different between each of the four *essC* variants. The regions spanning *essC* to the conserved gene *SAOUHSC_00279* were aligned between RN6390, and a. ST398 (*essC2* variant), b. MRSA252 (*essC3* variant) and c. HO 5096 0412 (*essC4* variant). Alignments were visualised using genoPlotR. d. A maximum likelihood tree constructed with IQTREE and annotated in iTOL for all *esaG* homologues found across the four representative *essC* variant strains RN6390, ST398, MRSA252 and HO 5096 0412.

Figure 6. Homologues of *tsaI* encoded at the *tspA* locus of RN6390. a. Genetic arrangement of *tsaI* genes in RN6390. *rclA* and *iolS* are a conserved gene found flanking the TspA locus in *S. aureus* strains, encoding a pyridine nucleotide-disulfide oxidoreductase and an aldo-keto reductase, respectively. b. An alignment of the encoded TsaI homologues. The black boxes represent regions of high homology based in this alignment. c. Alignment of the intergenic region downstream of each *tsaI* gene.

Figure 7. Assessing recombination events within *tsaI* homologues. a. A single region of high homology across the RN6390 TsaI protein sequences (middle panel) and the corresponding nucleotide sequences (bottom panel). The numbers which dictate the limits of the conserved region are taken form the nucleotide sequence of *tsaI1*. b. RDP4 was used to predict recombination events within the *tsaI* homologues encoded in RN6390. Each gene is labelled in black, with regions of recombination labelled directly below in the colour of the gene from which the recombinant section originated.

Figure 8. *tsaI* genes are carried on Staphylococcal plasmids. The *tsaI*-encoding regions of unnamed plasmids from *S. simulans* MR1 (accession NZ_CP015643), *S. caprae* 26D (accession NZ_CP031272), *S. warneri* SWO (accession NZ_CP033101), along with plasmids pCAPBN21 (accession NZ_CP042342) and pSB1-57-a (accession CP070965) are shown.

Figure 9. Homologues of *tipC* encoded at the *telC* locus of *Streptococcus mitis* BCC08. a. Genetic arrangement of *tipC* genes in *S. mitis* BCC08. B. An alignment of the encoded TipC homologues. The blue boxes represent regions of high sequence homology, and the dashed line at the N-terminus of the aligned sequences indicates a probable lipoprotein signal peptide.

Figure 10. Recombination within the *S. mitis* BCC08 *tipC* homologues. a. Regions of high homology across the *S. mitis* BCC08 TipC protein sequences (middle panel) and the corresponding nucleotide sequences (bottom panel). The positions of blocks of high homology are shown in grey shading, with their relative positions along the gene sequence (top). The first 18 amino acids of TipC form a predicted lipoprotein signal sequence which is indicated by pale grey shading. The basepair positions that define the conserved regions are taken from the nucleotide sequences of *D8786_RS05940*. b. RDP4 was used to predict recombination events within the *tipC* homologues. The identity of each gene is given in black at the left, with regions of recombination labelled directly below, in the colour of the gene from which the recombinant section originated. c. A maximum likelihood tree was generated for *tipC* homologues in IQTREE and visualised and annotated in iTOL. d. The conserved (cyan) and variable (orange) regions of TipC were mapped to the crystal structure of *S. intermedius* TipC2 (pdb:6DHX; 53).

Figure S1. Similarity plots for representative EsaG and TsaI amino acid sequences. All available amino acid sequences for EsaG and TsaI were obtained from RefSeq. Sequences were aligned and a similarity plot produced using plotcon for a. EsaG and b. TsaI.

Figure S2. Homology in the intergenic regions downstream of *esaG*genes in RN6390. a. The intergenic regions found directly downstream of each *esaG* gene were aligned and visualised using boxshade. b. Plotcon analysis of RN6390 *esaG* genes and their 3' intergenic regions. Alignment of *esaG* nucleotide sequences including the downstream IGR for *esaG*

574 genes from RN6390. e*saG1, esaG5 and esaG12* were excluded due to having a longer
575 intergenic region (as seen in Fig S2a). c. Nucleotide sequence alignment
576 for *esaG2* (NCTC8325_00242) and *esaG8 (NCTC8325_00250)* from NCTC8325-Sanger
577 with *SAOUHSC_00274* from NCTC8325-Oklahoma. d. Schematic representation of the
578 mosaic nature of *SAOUHSC_00274*.
579
580 **Figure S3. Alignment of the nucleotide sequences of *esD1-esaD12*.** The blocks of high
581 sequence homology corresponding to Fig 4a are outlined in blue.
582
583 **Figure S4. A recombination event in an epidemic lineage of USA300 results in loss of**
584 **part of an *esaG* cluster and generation of a novel *esaG* gene.** a. The *esaD* locus of
585 USA300 FPR3757 and USA300 BKV_2. The dashed lines represent the region that is missing
586 from the epidemic strain, USA300 BKV_2, when compared to the USA300 FPR3757 type
587 strain. b. Nucleotide sequence alignment for *SAUSA300_0295* and *SAUSA300_0299* from
588 USA300 FPR3757 and *esaG4* from USA300 BKV_2. Coloured blocks indicated homology
589 between *BKV_2 esaG4* and the genes with which it is aligned.
590
591 **Figure S5. Assessing recombination events in *esaG* homologues from a representative**
592 ***essC2*, *essC3* and *essC4* strain.** Alignments of *esaG* homologues from RN6390 with a.
593 ST398 (*essC2* variant), b. MRSA252 (*essC3* variant) and c. HO 5096 0412 (*essC4* variant)
594 were analysed using RDP4 to analyse recombination events. Each gene is labelled in black,
595 with regions of recombination labelled directly below in the colour of the gene from which the
596 recombinant section originated.
597
598 **Figure S6. Representation of the variability in the numbers of *tsaI* homologues encoded**
599 **by *S. aureus* strains.** Homologues of TsaI1 were obtained from RefSeq and genes
600 neighbouring the *tsaI* genes were identified - a selection of strains were used to visualise the
601 variability in number of *tsaI* genes encoded at this locus.

Figure S7. Alignment of the nucleotide sequences of *tsal1-tsal11* from RN6390. The block of high sequence homology corresponding to Fig 7a is outlined in blue.

Figure S8. Alignment of the nucleotide sequences of *tipC* homologues from *S. mitis* BCC08. The blocks of high sequence homology corresponding to Fig 9a are outlined in blue. The region encoding the predicted lipoprotein signal peptide is indicated with a dashed line.

Table S1. SNP table for NCTC_8325-Oklahoma compared to NCTC8325-Sanger. Large deletions and insertions are included below.

Table S2. SNP table for NCTC_8325-Oklahoma compared to RN6390.

Table S3. SNP table for NCTC_8325-Sanger compared to RN6390.

Table S4. RDP4 output for recombination within the *esaG* genes from RN6390. Predicted recombination events are highlighted in blue. Events that may have occurred due to an evolutionary process other than recombination are highlighted in yellow.

Table S5. RDP4 output for recombination within the *esaG* genes from RN6390 and ST398. Predicted recombination events are highlighted in blue.

Table S6. RDP4 output for recombination within the *esaG* genes from RN6390 and MRSA252. Predicted recombination events are highlighted in blue. Events that may have occurred due to an evolutionary process other than recombination are highlighted in yellow.

628 **Table S7. RDP4 output for recombination within the *esaG* genes from RN6390 and HO**
629 **5096 0412.** Predicted recombination events are highlighted in blue. Events that may have
630 occurred due to an evolutionary process other than recombination are highlighted in yellow.
631
632 **Table S8. RDP4 output for recombination within the *tsaI* genes from RN6390.** Events that
633 may have occurred due to an evolutionary process other than recombination are highlighted
634 in yellow.
635
636 **Table S9. RDP4 output for recombination within the *tipC* genes from *S. mitis* BCC08.**
637 Predicted recombination events are highlighted in blue. Events that may have occurred due
638 to an evolutionary process other than recombination are highlighted in yellow.

References

1. **Hsu T, Hingley-Wilson SM, Chen B, Chen M, Dai AZ *et al.*** The primary mechanism of attenuation of bacillus Calmette-Guerin is a loss of secreted lytic function required for invasion of lung interstitial tissue. *Proc Natl Acad Sci U S A* 2003;100:12420-12425.

2. **Pym AS, Brodin P, Majlessi L, Brosch R, Demangel C, *et al.*** Recombinant BCG exporting ESAT-6 confers enhanced protection against tuberculosis. Nat Med 2003;9:533-539.

3. **Stanley SA, Raghavan S, Hwang WW, Cox JS.** Acute infection and macrophage subversion by *Mycobacterium tuberculosis* require a specialized secretion system. *Proc Natl Acad Sci U S A* 2003;100:13001-13006.

4. **Akpe San Roman S, Facey PD, Fernandez-Martinez L, Rodriguez C, Vallin C *et al*.** A heterodimer of EsxA and EsxB is involved in sporulation and is secreted by a type VII secretion system in *Streptomyces coelicolor*. *Microbiology* 2010;156:1719-1729.

5. **Burts ML, Williams WA, DeBord K, Missiakas DM.** EsxA and EsxB are secreted by an ESAT-6-like system that is required for the pathogenesis of *Staphylococcus aureus* infections. *Proc Natl Acad Sci U S A* 2005;102:1169-1174.

6. **Bunduc CM, Fahrenkamp D, Wald J, Ummels R, Bitter W *et al*.** Structure and dynamics of a mycobacterial type VII secretion system. *Nature* 2021;593:445-448.

7. **Beckham KSH, Ritter C, Chojnowski G, Ziemianowicz DS, Mullapudi E *et al*.** Structure of the mycobacterial ESX-5 type VII secretion system pore complex. *Sci Adv* 2021;7:eabg9923.

8. **Abdallah AM, Gey van Pittius NC, Champion PA, Cox J, Luirink J, *et al.*** Type VII secretion--mycobacteria show the way. *Nat Rev Microbiol* 2007;5:883-891.

9. **Zoltner M, Ng WM, Money JJ, Fyfe PK, Kneuper H, *et al.*** EssC: domain structures inform on the elusive translocation channel in the Type VII secretion system. *Biochem J* 2016; 473:1941-1952.

10. **Bowman L, Palmer T.** The Type VII Secretion System of *Staphylococcus*. *Annu Rev Microbiol* 2021;75:471-494.

11. **Tran HR, Grebenc DW, Klein TA, Whitney JC.** Bacterial type VII secretion: An important player in host-microbe and microbe-microbe interactions. *Mol Microbiol* 2021;115:478-489.

12. **Whitney JC, Peterson SB, Kim J, Pazos M, Verster AJ, *et al.*** A broadly distributed toxin family mediates contact-dependent antagonism between gram-positive bacteria. *Elife*. 2017; 6:e26938.

13. **Chatterjee A, Willett JLE, Dunny GM, Duerkop BA.** Phage infection and sub-lethal antibiotic exposure mediate *Enterococcus faecalis* type VII secretion system dependent inhibition of bystander bacteria. *PLoS genet* 2021;17:e1009204.

14. **Bowran K, Palmer T.** Extreme genetic diversity in the type VII secretion system of Listeria monocytogenes suggests a role in bacterial antagonism. *Microbiology* 2021;167: doi: 10.1099/mic.0.001034

15. **Cao Z, Casabona MG, Kneuper H, Chalmers JD, Palmer T.** The type VII secretion system of *Staphylococcus aureus* secretes a nuclease toxin that targets competitor bacteria. *Nat Microbiol* 2016;2:16183.

16. **Warne B, Harkins CP, Harris SR, Vatsiou A, Stanley-Wall N, *et al.*** The Ess/Type VII secretion system of *Staphylococcus aureus* shows unexpected genetic diversity. *BMC Genomics* 2016;17:222.

17. **Baek KT, Frees D, Renzoni A, Barras C, Rodriguez N *et al*.** Genetic variation in the *Staphylococcus aureus* 8325 strain lineage revealed by whole-genome sequencing. PLoS ONE. 2013;8:e77122.

18. **Ohr RJ, Anderson M, Shi M, Schneewind O, Missiakas D.** EssD, a Nuclease Effector of the *Staphylococcus aureus* ESS Pathway. *J Bacteriol* 2016;199:e00528-16.

19. **Ulhuq FR, Gomes MC, Duggan GM, Guo M, Mendonca C, *et al.*** A membrane-depolarizing toxin substrate of the *Staphylococcus aureus* Type VII secretion system mediates intra-species competition. *Proc Natl Acad Sci U S A* 2020;117:20836-20847.

20. **Ross BD, Verster AJ, Radey MC, Schmidtke DT, Pope CE *et al*.** Human gut bacteria contain acquired interbacterial defence systems. *Nature* 2019;575:224-228.

21. **Novick RP.** Genetic systems in staphylococci. *Methods Enzymol* 1991;204:587-636.

22. **Herbert S, Ziebandt AK, Ohlsen K, Schafer T, Hecker M *et al*.** Repair of global regulators in *Staphylococcus aureus* 8325 and comparative analysis with other clinical isolates. *Infect Immun* 2010;78:2877-2889.

23. **Novick R.** Properties of a cryptic high-frequency transducing phage in *Staphylococcus aureus*. Virology 1967;33:155-166.

24. **Peng HL, Novick RP, Kreiswirth B, Kornblum J, Schlievert P.** Cloning, characterization, and sequencing of an accessory gene regulator (*agr*) in *Staphylococcus aureus*. *J Bacteriol* 1988;170:4365-4372.

25. **Kneuper H, Cao ZP, Twomey KB, Zoltner M, Jäger F, *et al.*** Heterogeneity in ess transcriptional organization and variable contribution of the Ess/Type VII protein secretion system to virulence across closely related *Staphylocccus aureus* strains. *Mol Microbiol* 2014;93:928-943.

26. **Casabona MG, Kneuper H, Alferes de Lima D, Harkins CP, Zoltner M *et al*.** Haem-iron plays a key role in the regulation of the Ess/type VII secretion system of *Staphylococcus aureus* RN6390. *Microbiology* 2017;163:1839-1850.

27. **Gillaspy AF, Worrell V, Orvis J, Roe BA, Dyer DW, Iandolo JJ.** *Staphylococcus aureus* NCTC8325 genome. In: Fischetti V, Novick R, Ferretti J, Portnoy D, Rood J, editors. Gram-positive pathogens. Washington, D.C.: ASM Press; 2006. p. 381-412.

28. **Darling AE, Mau B, Perna NT.** progressiveMauve: multiple genome alignment with gene gain, loss and rearrangement. *PLoS ONE* 2010;5:e11147.

29. **Seemann T.** snippy: fast bacterial variant calling from NGS reads https://github.com/tseemann/snippy. 2015.

30. **Nishimura Y, Yoshida T, Kuronishi M, Uehara H, Ogata H, Goto S.** ViPTree: the viral proteomic tree server. *Bioinformatics* 2017;33:2379-2380.

31. **Katoh K, Misawa K, Kuma K, Miyata T.** MAFFT: a novel method for rapid multiple sequence alignment based on fast Fourier transform. *Nucleic Acids Res* 2002;30:3059-3066.

32. **Edgar RC.** MUSCLE: multiple sequence alignment with high accuracy and high throughput. *Nucleic Acids Res* 2004;32:1792-1797.

33. **Martin DP, Murrell B, Golden M, Khoosal A, Muhire B.** RDP4: Detection and analysis of recombination patterns in virus genomes. *Virus Evol* 2015;1:vev003.

34. **Capella-Gutierrez S, Silla-Martinez JM, Gabaldon T.** trimAl: a tool for automated alignment trimming in large-scale phylogenetic analyses. *Bioinformatics* 2009;25:1972-1973.

35. **Minh BQ, Schmidt HA, Chernomor O, Schrempf D, Woodhams MD *et al*.** IQ-TREE 2: New models and efficient methods for phylogenetic inference in the genomic era. Mol Biol Evol 2020;37:1530-1534.

36. **Letunic I, Bork P.** Interactive Tree Of Life (iTOL) v5: an online tool for phylogenetic tree display and annotation. *Nucleic Acids Res* 2021;49:W293-W6.

37. **Altschul SF, Gish W, Miller W, Myers EW, Lipman DJ.** Basic local alignment search tool. *J Mol Biol* 1990;215:403-410.

38. **Guy L, Kultima JR, Andersson SG.** genoPlotR: comparative gene and genome visualization in R. *Bioinformatics* 2010;26**:**2334-2335.

39. **RStudio Team.** RStudio: Integrated Development for R. RStudio, PBC, Boston, MA URL http://www.rstudio.com/ 2020.

40. **Saha CK, Sanches Pires R, Brolin H, Delannoy M, Atkinson GC.** FlaGs and webFlaGs: discovering novel biology through the analysis of gene neighbourhood conservation. *Bioinformatics* 2021;37:1312-1314.

41. **Galata V, Fehlmann T, Backes C, Keller A.** PLSDB: a resource of complete bacterial plasmids. *Nucleic Acids Res* 2019;47:D195-D202.

42. **Eddy SR.** Accelerated profile HMM searches. *PLoS Comput Biol* 2011;7:e1002195.

786 43. **Coordinators NR.** Database resources of the National Center for biotechnology
787 information. Nucleic Acids Res 2017;45:D12–17.
788
789 44. **Goerke C, Wirtz C, Fluckiger U, Wolz C.** Extensive phage dynamics in *Staphylococcus*
790 *aureus* contributes to adaptation to the human host during infection. *Mol Microbiol*
791 2006;61:1673-1685.
792
793 45**. Goerke C, Pantucek R, Holtfreter S, Schulte B, Zink M *et al*.** Diversity of prophages in
794 dominant *Staphylococcus aureus* clonal lineages. J Bacteriol 2009;191:3462-3468.
795
796 46. **Seybold U, Kourbatova EV, Johnson JG, Halvosa SJ, Wang YF *et al*.** Emergence of
797 community-associated methicillin-resistant *Staphylococcus aureus* USA300 genotype as a
798 major cause of health care-associated blood stream infections. *Clin Infect Dis* 2006;42:647-
799 656.
800
801 47. **Copin R, Sause WE, Fulmer Y, Balasubramanian D, Dyzenhaus S *et al*.** Sequential
802 evolution of virulence and resistance during clonal spread of community-acquired methicillin-
803 resistant Staphylococcus aureus. *Proc Natl Acad Sci U S A* 2019;116:1745-1754.
804
805 48. **Guy L, Kultima JR, Andersson SG.** genoPlotR: comparative gene and genome
806 visualization in R. *Bioinformatics* 2010;26:2334-2335.
807
808 49. **Arnold BJ, Huang IT, Hanage WP.** Horizontal gene transfer and adaptive evolution in
809 bacteria. *Nat Rev Microbiol* 2021 in press doi: 10.1038/s41579-021-00650-4.
810
811 50. **Stevenson C, Hall JP, Harrison E, Wood A, Brockhurst MA.** Gene mobility promotes
812 the spread of resistance in bacterial populations. *ISME J* 2017;11:1930-1932.
813
814 51. **Buckner MMC, Ciusa ML, Piddock LJV.** Strategies to combat antimicrobial resistance:
815 anti-plasmid and plasmid curing. *FEMS Microbiol Rev* 2018;42:781-804.
816
817 52. **Zhang D, de Souza RF, Anantharaman V, Iyer LM, Aravind L.** Polymorphic toxin
818 systems: Comprehensive characterization of trafficking modes, processing, mechanisms of
819 action, immunity and ecology using comparative genomics. *Biol Direct* 2012;7:18.
820

821 53. **Klein TA, Pazos M, Surette MG, Vollmer W, Whitney JC.** Molecular Basis for Immunity
822 Protein Recognition of a Type VII Secretion System Exported Antibacterial Toxin. *J Mol Biol*
823 2018;430:4344-4358.
824
825 54. **Michel B, Leach D.** Homologous Recombination-Enzymes and Pathways. *EcoSal Plus*
826 2012;5: doi: 10.1128/ecosalplus.7.2.7.
827
828 55. **Khasanov FK, Zvingila DJ, Zainullin AA, Prozorov AA, Bashkirov VI.** Homologous
829 recombination between plasmid and chromosomal DNA in *Bacillus subtilis* requires
830 approximately 70 bp of homology. *Mol Gen Genet* 1992;234:494-497.
831
832 56. **Shen P, Huang HV.** Homologous recombination in *Escherichia coli*: dependence on
833 substrate length and homology. *Genetics* 1986;112:441-457.
834
835 57. **Fujitani Y, Yamamoto K, Kobayashi I.** Dependence of frequency of homologous
836 recombination on the homology length. *Genetics* 1995;140:797-809.
837
838 58. **Tsuru T, Kawai M, Mizutani-Ui Y, Uchiyama I, Kobayashi I.** Evolution of paralogous
839 genes: Reconstruction of genome rearrangements through comparison of multiple genomes
840 within *Staphylococcus aureus*. *Mol Biol Evol* 2006;23:1269-1285.
841
842 59. **Tsuru T, Kobayashi I.** Multiple genome comparison within a bacterial species reveals a
843 unit of evolution spanning two adjacent genes in a tandem paralog cluster. *Mol Biol Evol*
844 2008;25:2457-2473.
845
846 60. **Ruhe ZC, Low DA, Hayes CS.** Polymorphic Toxins and Their Immunity Proteins:
847 Diversity, Evolution, and Mechanisms of Delivery. *Annu Rev Microbiol* 2020;74:497-520.
848
849 61. **Diep DB, Skaugen M, Salehian Z, Holo H, Nes IF.** Common mechanisms of target cell
850 recognition and immunity for class II bacteriocins. *Proc Natl Acad Sci U S A* 2007;104:2384-
851 2389.
852
853 62. **Kreiswirth BN, Lofdahl S, Betley MJ, O'Reilly M, Schlievert PM *et al*.** The toxic shock
854 syndrome exotoxin structural gene is not detectably transmitted by a prophage. *Nature*
855 1983;305:709-712.
856

857 63. **Novick RP.** Studies on plasmid replication. III. Isolation and characterization of replication-
858 defective mutants. *Mol Gen Genet* 1974;135:131-147.
859
860 64. **Pattee PA.** Distribution of Tn551 insertion sites responsible for auxotrophy on the
861 *Staphylococcus aureus* chromosome. *J Bacteriol* 1981;145:479-488.
862
863

a

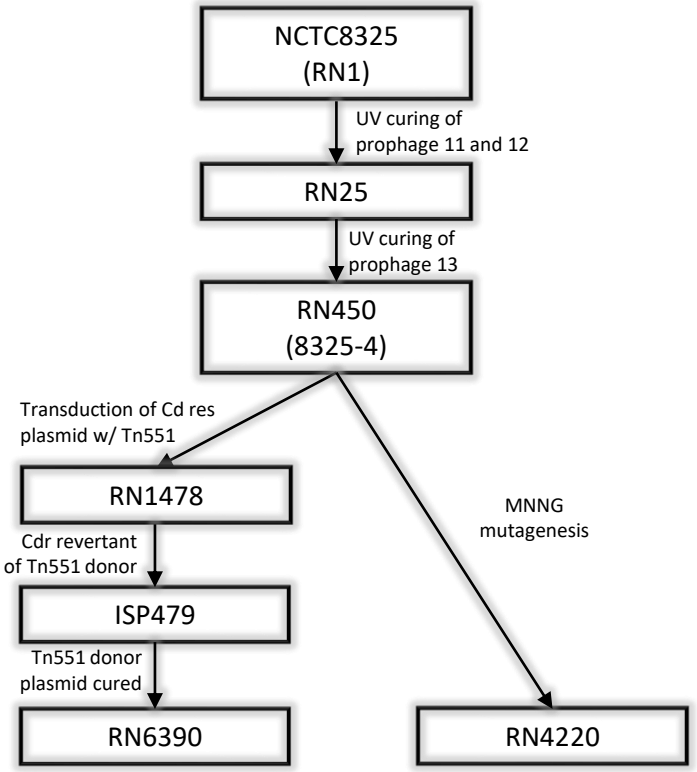
NCTC8325
(RN1)
UV curing of
prophage 11 and 12
RN25
UV curing of
prophage 13
RN450
(8325-4)
Transduction of Cd res
plasmid w/ Tn551
RN1478
MNNG
mutagenesis
Cdr revertant
of Tn551 donor
ISP479
Tn551 donor
plasmid cured
RN6390
RN4220

b

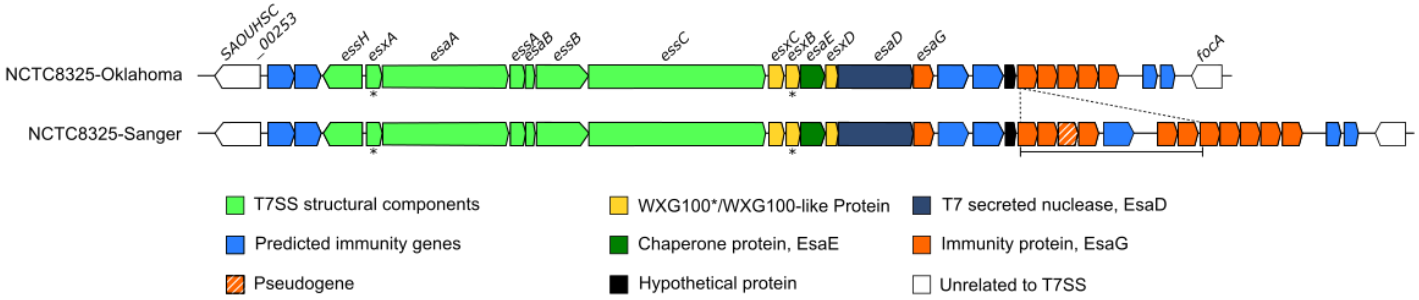
SAOUHSC_00253
essH
esxA
esaA
essA
esaB
essB
essC
esxC
esxB
esaE
esxD
esaD
esaG
focA
NCTC8325-Oklahoma
NCTC8325-Sanger
T7SS structural components
Predicted immunity genes
Pseudogene
WXG100*/WXG100-like Protein
Chaperone protein, EsaE
Hypothetical protein
T7 secreted nuclease, EsaD
Immunity protein, EsaG
Unrelated to T7SS

Fig 1

a

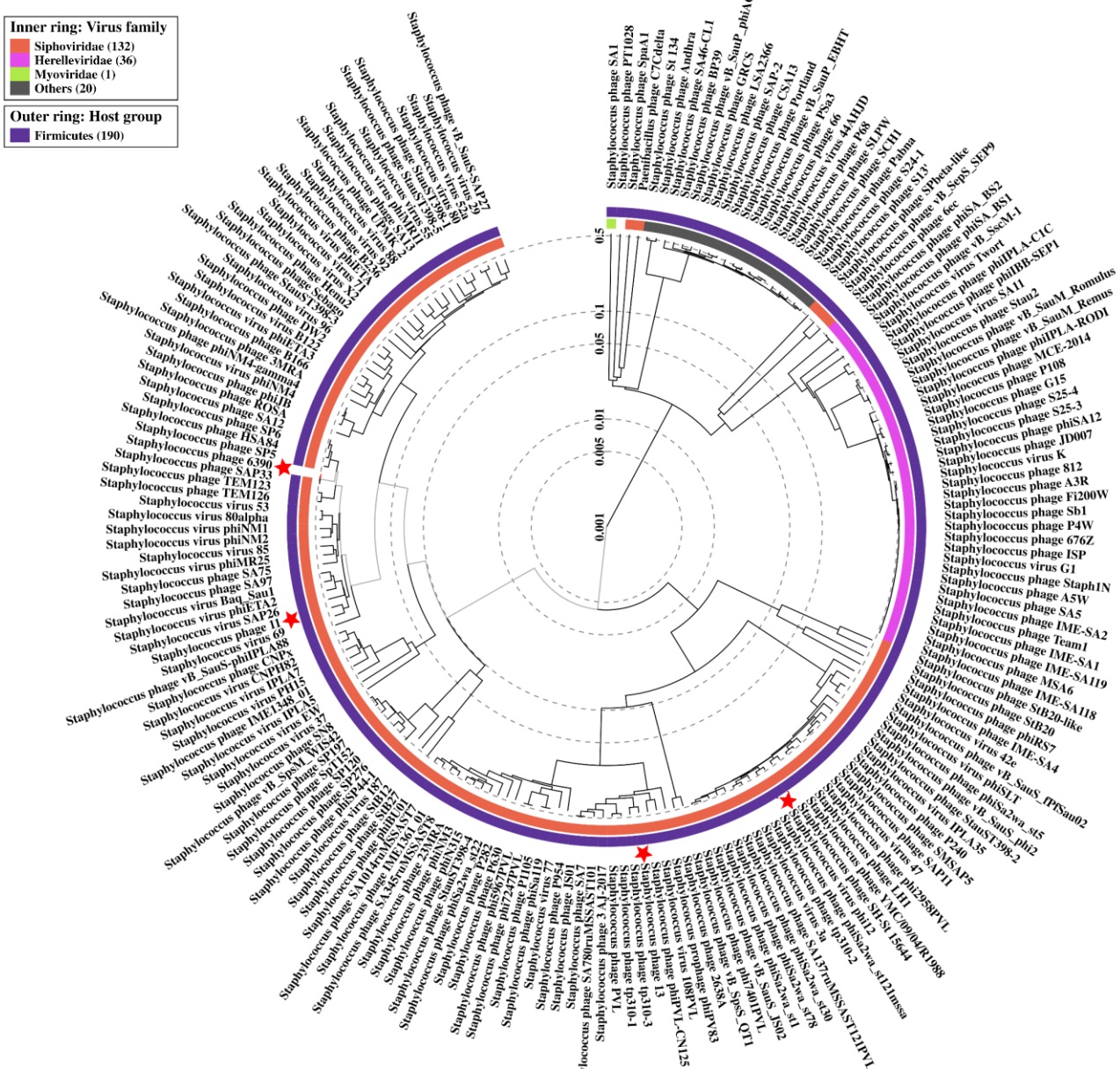
Inner ring: Virus family
Siphoviridae (132)
Herelleviridae (36)
Myoviridae (1)
Others (20)
Outer ring: Host group
Firmicutes (190)
0.5
0.1
0.05
0.01
0.005
0.001

Fig 2

a

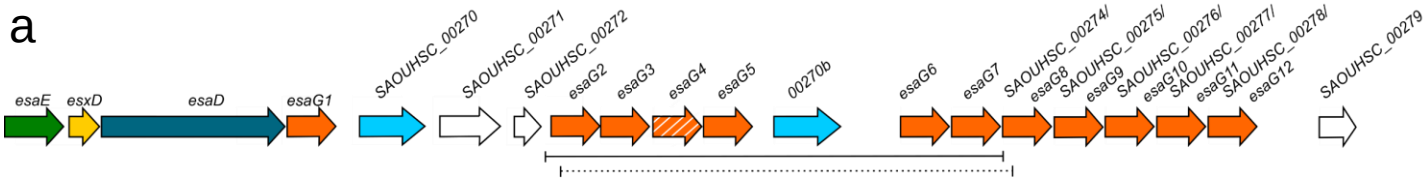
esaE
esxD
esaD
esaG1
SAOUHSC_00270
SAOUHSC_00271
SAOUHSC_00272
esaG2
esaG3
esaG4
esaG5
00270b
esaG6
esaG7
SAOUHSC_00274
esaG8
SAOUHSC_00275
esaG9
SAOUHSC_00276
esaG10
SAOUHSC_00277
esaG11
SAOUHSC_00278
esaG12
SAOUHSC_00279

b

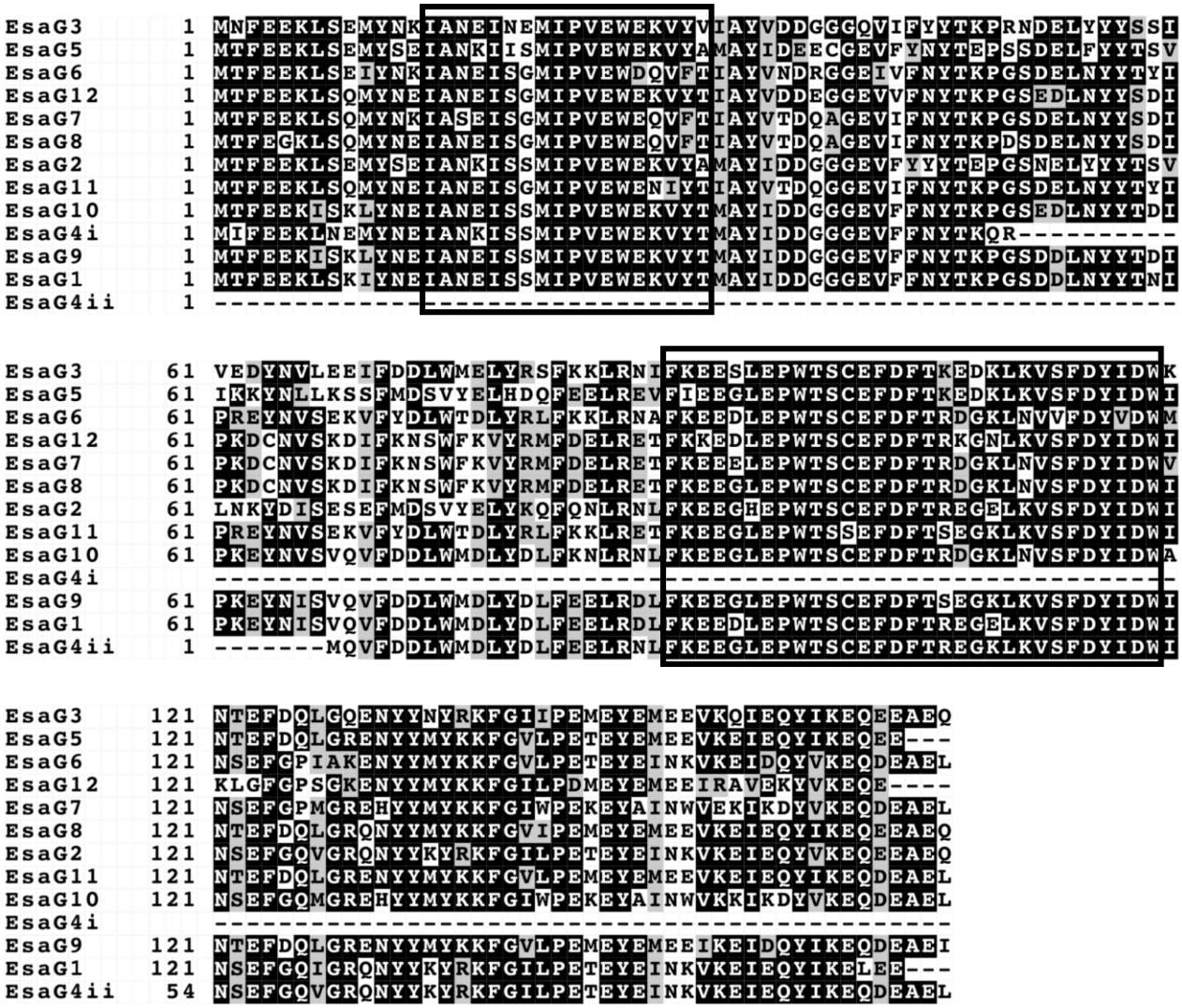
EsaG3 1 MNFEEKLSEMYNKIANEINEMIPVEWEKVYVIAYVDDGGQVIFYYTKPRNDELYYYSSI
EsaG5 1 MTFEEKLSEMYSEIANKIISMIPVEWEKVYAMAYIDEECGEVFYNYTEPSSDELFYYTSV
EsaG6 1 MTFEEKLSEIYNKIANEISGMIPVEWDQVFTIAYVNDRGGEIVFNYTKPGSDELNYYTYI
EsaG12 1 MTFEEKLSQMYNEIANEISGMIPVEWEKVYTIAYVDDEGGEVVFNYTKPGSEDLNYYSDI
EsaG7 1 MTFEEKLSQMYNKIASEISGMIPVEWEQVFTIAYVTDQAGEVIFNYTKPGSDELNYYSDI
EsaG8 1 MTFEGKLSQMYNEIANEISGMIPVEWEQVFTIAYVTDQAGEVIFNYTKPDSDELNYYSDI
EsaG2 1 MTFEEKLSEMYSEIANKISSMIPVEWEKVYAMAYIDDGGGEVFYYYTEPGSNELYYYTSV
EsaG11 1 MTFEEKLSQMYNEIANEISGMIPVEWENIYTIAYVTDQGGEVIFNYTKPGSDELNYYTYI
EsaG10 1 MTFEEKISKLYNEIANEISSMIPVEWEKVYTMAYIDDGGGEVFFNYTKPGSEDLNYYTDI
EsaG4i 1 MIFEEKLNEMYNEIANKISSMIPVEWEKVYTMAYIDDGGGEVFFNYTKQR----------
EsaG9 1 MTFEEKISKLYNEIANEISSMIPVEWEKVYTMAYIDDGGGEVFFNYTKPGSDDLNYYTDI
EsaG1 1 MTFEEKLSKIYNEIANEISSMIPVEWEKVYTMAYIDDGGGEVFFNYTKPGSDDLNYYTNI
EsaG4ii 1 ----------MQVFDDLWMDLYDLFEELRNLFKEEGLEPWTSCEFDFTREGKLKVSFDYIDWI
EsaG3 61 VEDYNVLEEIFDDLWMELYRSFKKLRNIFKEESLEPWTSCEFDFTKEDKLKVSFDYIDWK
EsaG5 61 IKKYNLLKSSFMDSVYELHDQFEELREVFIEEGLEPWTSCEFDFTKEDKLKVSFDYIDWI
EsaG6 61 PREYNVSEKVFYDLWTDLYRLFKKLRNAFKEEDLEPWTSCEFDFTRDGKLNVVFDYVDWM
EsaG12 61 PKDCNVSKDIFKNSWFKVYRMFDELRETFKKEDLEPWTSCEFDFTRKGNLKVSFDYIDWI
EsaG7 61 PKDCNVSKDIFKNSWFKVYRMFDELRETFKEEELEPWTSCEFDFTRDGKLNVSFDYIDWV
EsaG8 61 PKDCNVSKDIFKNSWFKVYRMFDELRETFKEEGLEPWTSCEFDFTRDGKLNVSFDYIDWI
EsaG2 61 LNKYDISESEFMDSVYELYKQFQNLRNLFKEEGHEPWTSCEFDFTREGELKVSFDYIDWI
EsaG11 61 PREYNVSEKVFYDLWTDLYRLFKKLRETFKEEGLEPWTSSEFDFTSEGKLKVSFDYIDWI
EsaG10 61 PKEYNVSVQVFDDLWMDLYDLFKNLRNLFKEEGLEPWTSCEFDFTRDGKLNVSFDYIDWA
EsaG4i ----------
EsaG9 61 PKEYNISVQVFDDLWMDLYDLFEELRDLFKEEGLEPWTSCEFDFTSEGKLKVSFDYIDWI
EsaG1 61 PKEYNISVQVFDDLWMDLYDLFEELRDLFKEEDLEPWTSCEFDFTREGELKVSFDYIDWI
EsaG4ii 1 -------MQVFDDLWMDLYDLFEELRNLFKEEGLEPWTSCEFDFTREGKLKVSFDYIDWI
EsaG3 121 NTEFDQLGQENYYNYRKFGIIPEMEYEMEEVKQIEQYIKEQEEAEQ
EsaG5 121 NTEFDQLGRENYYMYKKFGVLPETEYEMEEVKEIEQYIKEQEE---
EsaG6 121 NSEFGPIAKENYYMYKKFGVLPETEYEINKVKEIDQYVKEQDEAEL
EsaG12 121 KLGFGPSGKENYYMYKKFGILPDMEYEMEEIRAVEKYVKEQE----
EsaG7 121 NSEFGPMGREHYYMYKKFGIWPEKEYAINWVEKIKDYVKEQDEAEL
EsaG8 121 NTEFDQLGRQNYYMYKKFGVIPEMEYEMEEVKEIEQYIKEQEEAEQ
EsaG2 121 NSEFGQVGRQNYYKYRKFGILPETEYEINKVKEIEQYVKEQEEAEQ
EsaG11 121 NTEFDQLGRENYYMYKKFGVLPEMEYEMEEVKEIEQYIKEQDEAEL
EsaG10 121 NSEFGQMGREHYYMYKKFGIWPEKEYAINWVKKIKDYVKEQDEAEL
EsaG4i ----------
EsaG9 121 NTEFDQLGRENYYMYKKFGVLPEMEYEMEEIKEIDQYIKEQDEAEI
EsaG1 121 NSEFGQIGRQNYYKYRKFGILPETEYEINKVKEIEQYIKELEE---
EsaG4ii 54 NSEFGQVGRQNYYKYRKFGILPETEYEINKVKEIEQYIKEQDEAEL

Fig 3

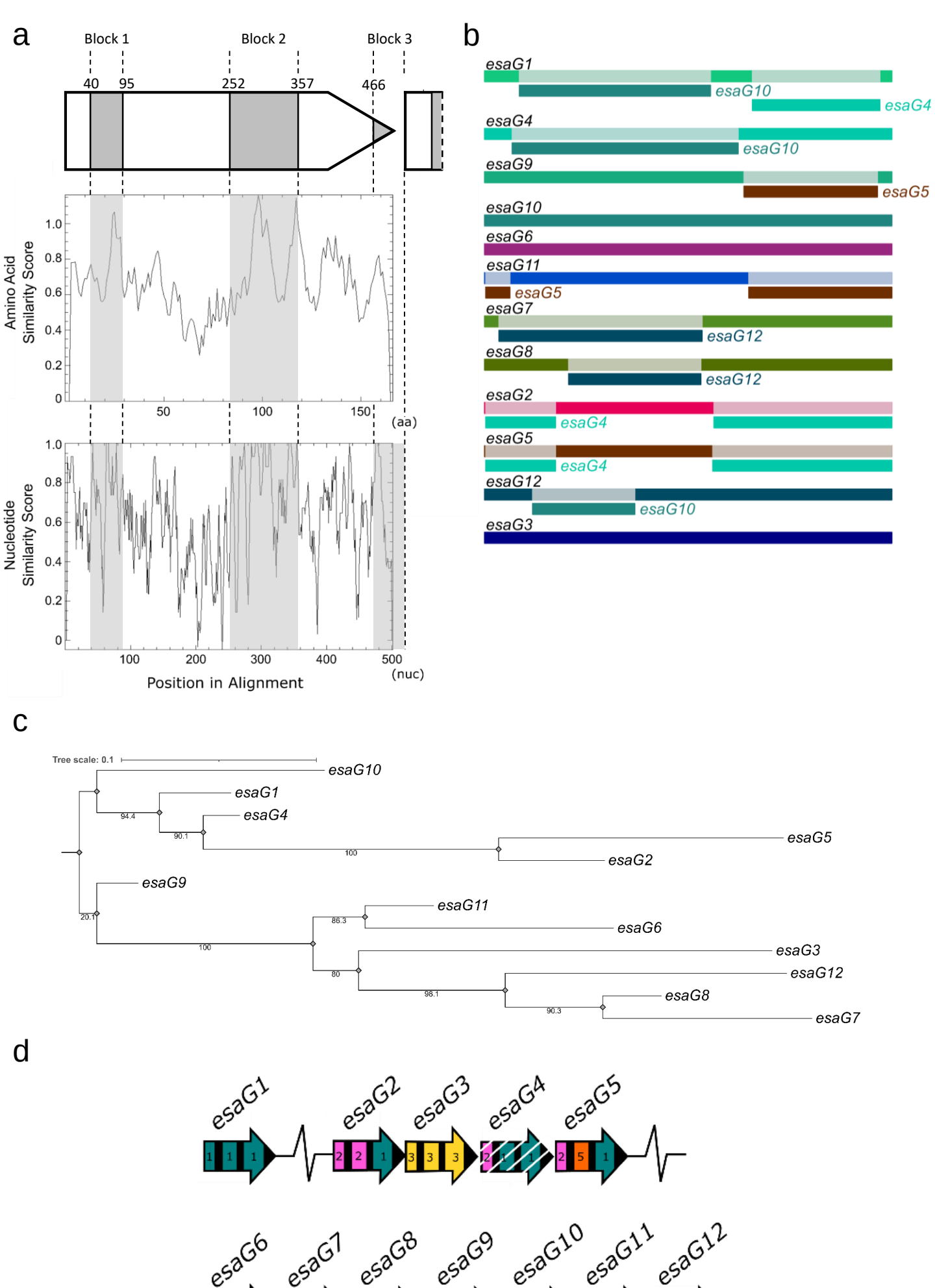
a
Block 1
Block 2
Block 3
40
95
252
357
466
Amino Acid Similarity Score
1.0
0.8
0.6
0.4
0.2
0
50
100
150
(aa)
Nucleotide Similarity Score
100
200
300
400
500
(nuc)
Position in Alignment
b
esaG1
esaG10
esaG4
esaG4
esaG10
esaG9
esaG5
esaG10
esaG6
esaG11
esaG5
esaG7
esaG12
esaG8
esaG12
esaG2
esaG4
esaG5
esaG4
esaG12
esaG10
esaG3
c
Tree scale: 0.1
esaG10
esaG1
esaG4
esaG5
esaG2
esaG9
esaG11
esaG6
esaG3
esaG12
esaG8
esaG7
94.4
90.1
100
20.1
86.3
100
80
98.1
90.3
d
esaG1
esaG2
esaG3
esaG4
esaG5
esaG6
esaG7
esaG8
esaG9
esaG10
esaG11
esaG12

Fig 4

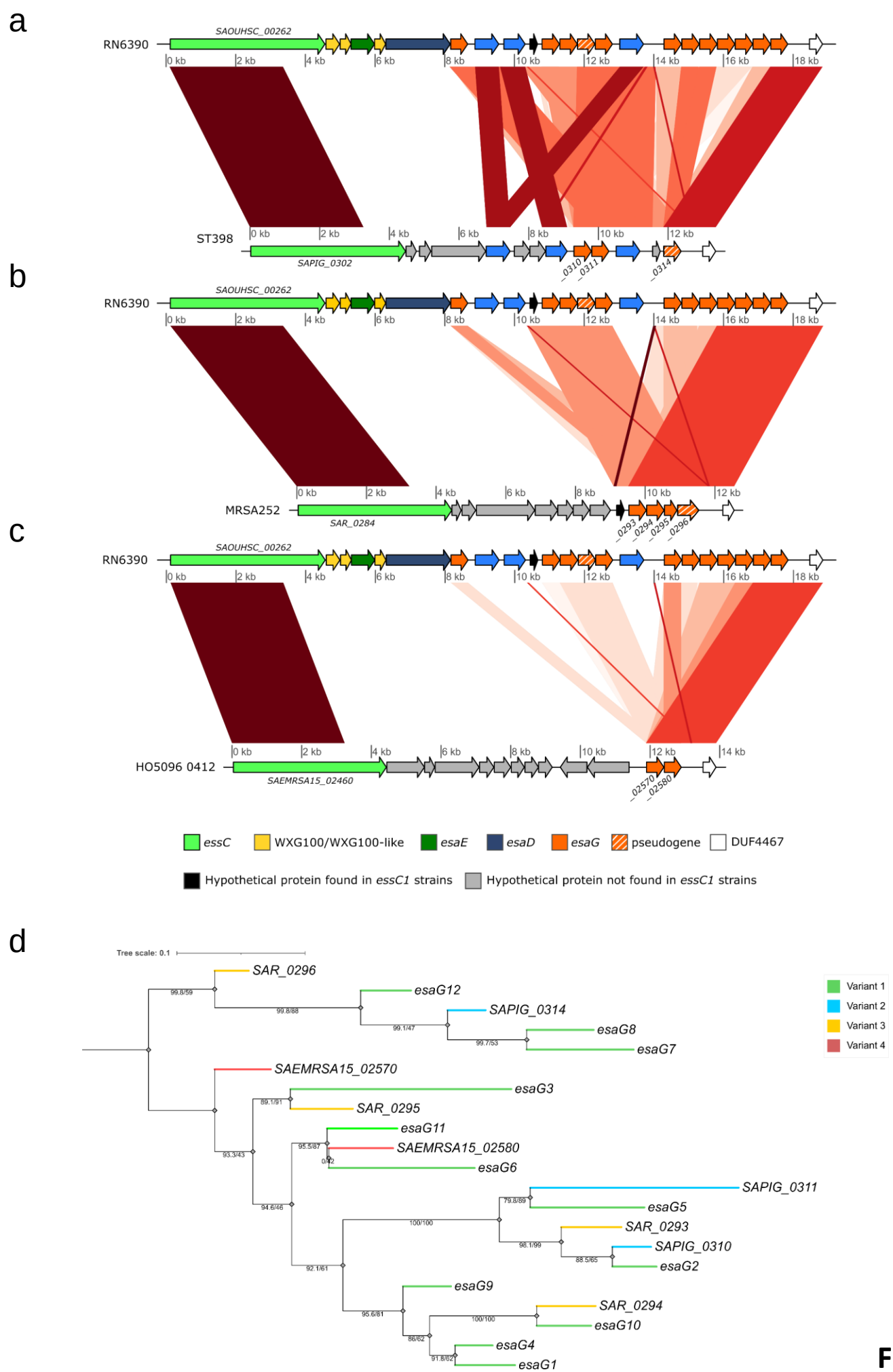
a
RN6390
SAOUHSC_00262
0 kb
2 kb
4 kb
6 kb
8 kb
10 kb
12 kb
14 kb
16 kb
18 kb
ST398
SAPIG_0302
_0310
_0311
_0314
b
RN6390
SAOUHSC_00262
MRSA252
SAR_0284
_0293
_0294
_0295
_0296
c
RN6390
SAOUHSC_00262
HO5096 0412
SAEMRSA15_02460
_02570
_02580
essC
WXG100/WXG100-like
esaE
esaD
esaG
pseudogene
DUF4467
Hypothetical protein found in essC1 strains
Hypothetical protein not found in essC1 strains
d
Tree scale: 0.1
SAR_0296
esaG12
SAPIG_0314
esaG8
esaG7
SAEMRSA15_02570
esaG3
SAR_0295
esaG11
SAEMRSA15_02580
esaG6
SAPIG_0311
esaG5
SAR_0293
SAPIG_0310
esaG2
esaG9
SAR_0294
esaG10
esaG4
esaG1
Variant 1
Variant 2
Variant 3
Variant 4

Fig 5

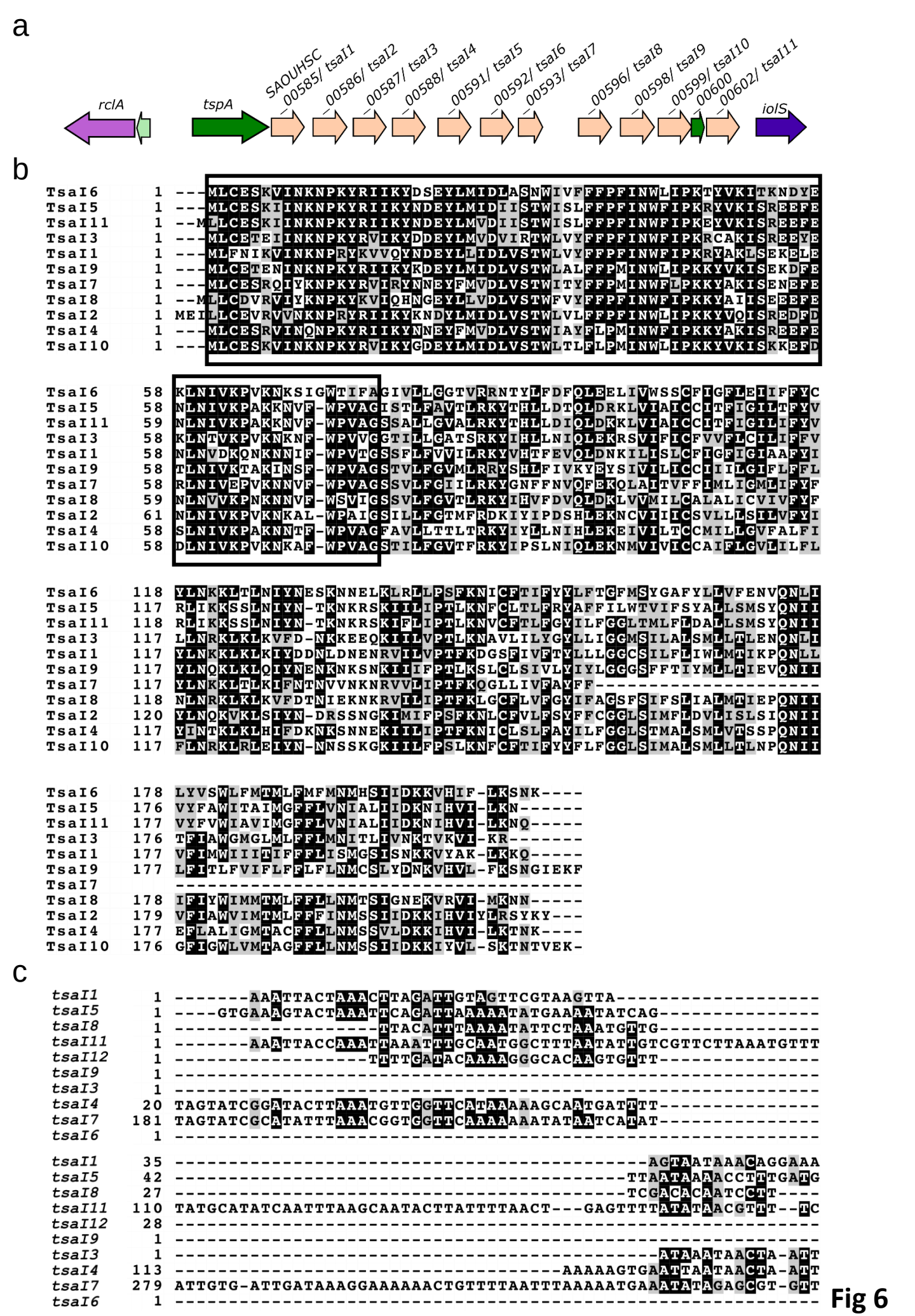
a
rclA
tspA
SAOUHSC_00585/ tsaI1
SAOUHSC_00586/ tsaI2
SAOUHSC_00587/ tsaI3
SAOUHSC_00588/ tsaI4
SAOUHSC_00591/ tsaI5
SAOUHSC_00592/ tsaI6
SAOUHSC_00593/ tsaI7
SAOUHSC_00596/ tsaI8
SAOUHSC_00598/ tsaI9
SAOUHSC_00599/ tsaI10
SAOUHSC_00600
SAOUHSC_00602/ tsaI11
iolS
b
TsaI6 TsaI5 TsaI11 TsaI3 TsaI1 TsaI9 TsaI7 TsaI8 TsaI2 TsaI4 TsaI10
c
tsaI1 tsaI5 tsaI8 tsaI11 tsaI12 tsaI9 tsaI3 tsaI4 tsaI7 tsaI6

Fig 6

a

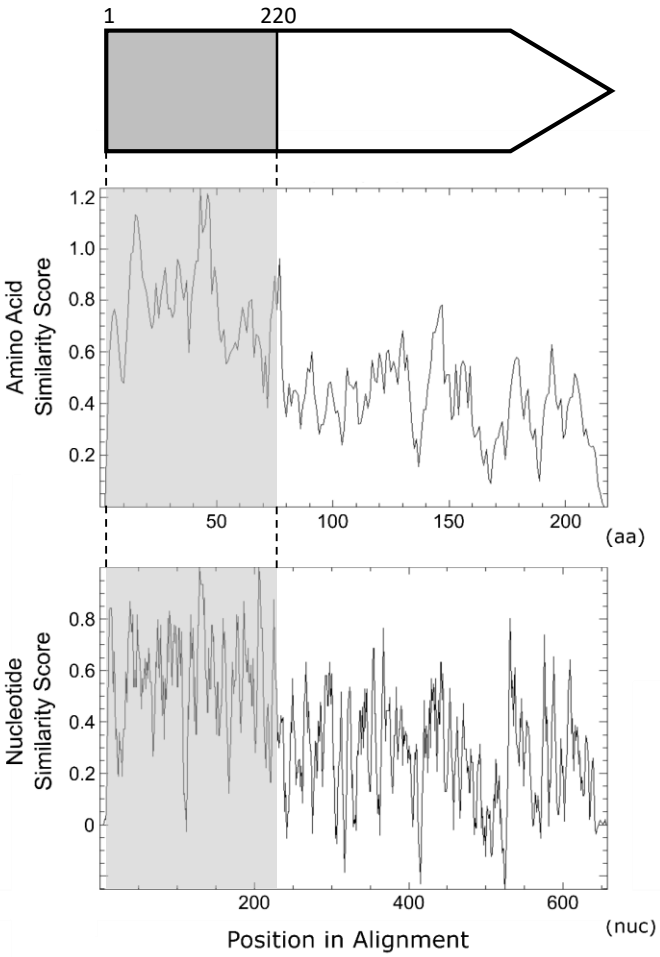
1
220
Amino Acid Similarity Score
1.2
1.0
0.8
0.6
0.4
0.2
50
100
150
200
(aa)
Nucleotide Similarity Score
0.8
0.6
0.4
0.2
0
200
400
600
(nuc)
Position in Alignment

b

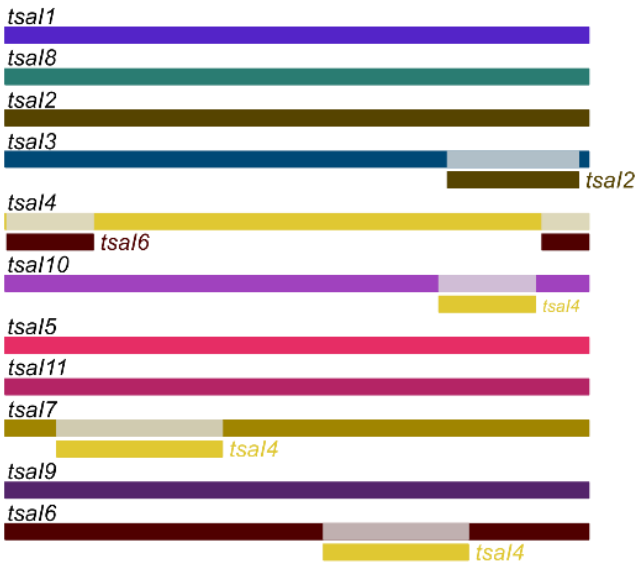
tsal1
tsal8
tsal2
tsal3
tsal2
tsal4
tsal6
tsal10
tsal4
tsal5
tsal11
tsal7
tsal4
tsal9
tsal6
tsal4

Fig 7

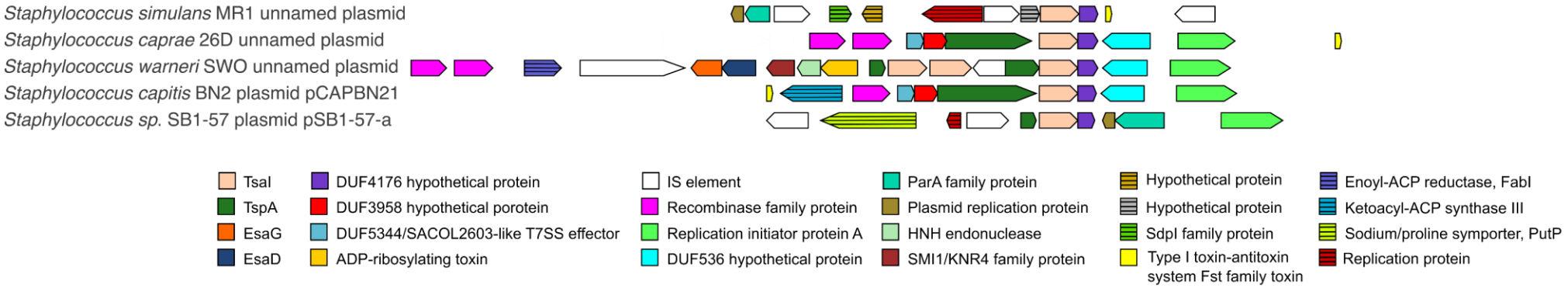
Staphylococcus simulans MR1 unnamed plasmid
Staphylococcus caprae 26D unnamed plasmid
Staphylococcus warneri SWO unnamed plasmid
Staphylococcus capitis BN2 plasmid pCAPBN21
Staphylococcus sp. SB1-57 plasmid pSB1-57-a
TsaI
TspA
EsaG
EsaD
DUF4176 hypothetical protein
DUF3958 hypothetical porotein
DUF5344/SACOL2603-like T7SS effector
ADP-ribosylating toxin
IS element
Recombinase family protein
Replication initiator protein A
DUF536 hypothetical protein
ParA family protein
Plasmid replication protein
HNH endonuclease
SMI1/KNR4 family protein
Hypothetical protein
Hypothetical protein
SdpI family protein
Type I toxin-antitoxin system Fst family toxin
Enoyl-ACP reductase, FabI
Ketoacyl-ACP synthase III
Sodium/proline symporter, PutP
Replication protein

Fig 8

a

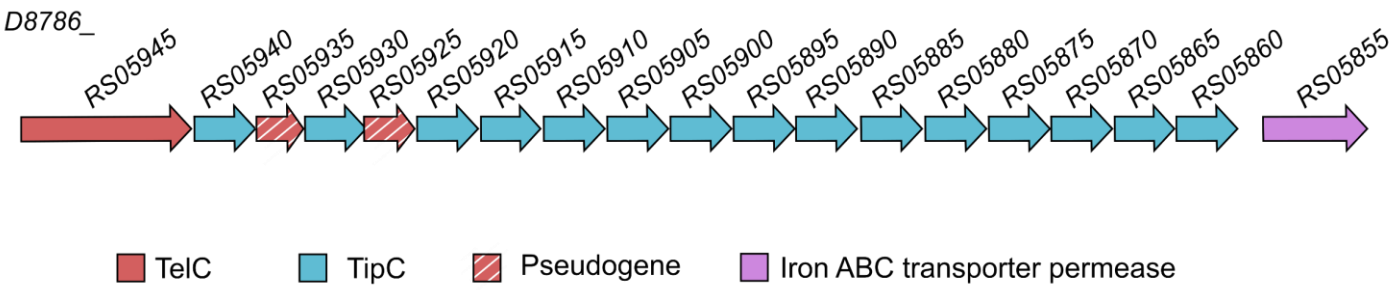
D8786_
RS05945
RS05940
RS05935
RS05930
RS05925
RS05920
RS05915
RS05910
RS05905
RS05900
RS05895
RS05890
RS05885
RS05880
RS05875
RS05870
RS05865
RS05860
RS05855
TelC
TipC
Pseudogene
Iron ABC transporter permease

b

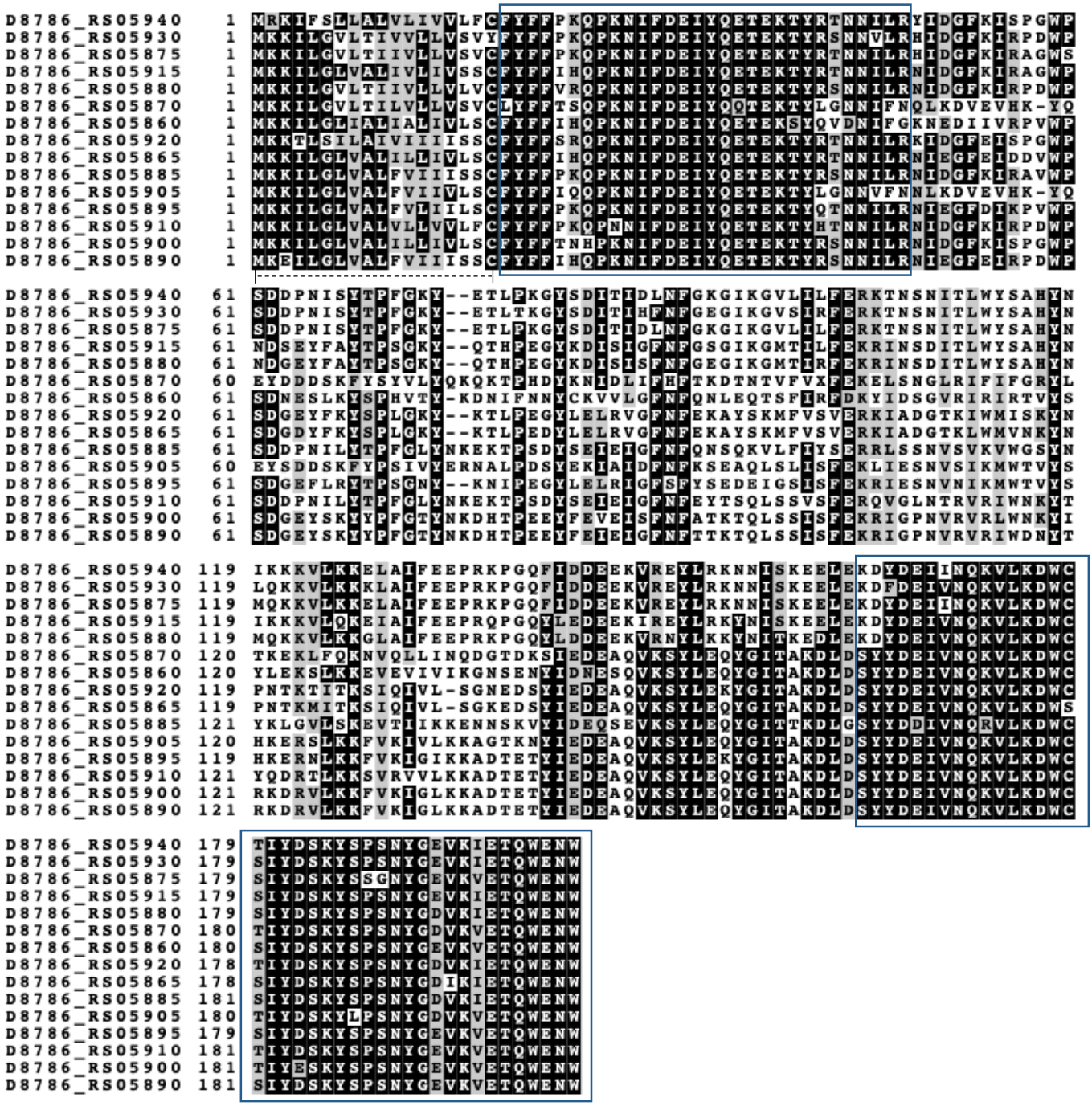
D8786_RS05940 1 MRKIFSLLALVLIVVLFCFYFFPKQPKNIFDEIYQETEKTYRTNNILRYIDGFKISPGWP
D8786_RS05930 1 MKKILGVLTIVVLLVSVYFYFFPKQPKNIFDEIYQETEKTYRSNNVLRHIDGFKIRPDWP
D8786_RS05875 1 MKKILGVLTIIVLLVSVCFYFFPKQPKNIFDEIYQETEKTYRTNNILRHIDGFKIRAGWS
D8786_RS05915 1 MKKILGLVALIVLIVSSCFYFFIHQPKNIFDEIYQETEKTYRTNNILRNIDGFKIRAGWP
D8786_RS05880 1 MKKILGVLTIIVLLVLVCFYFFVRQPKNIFDEIYQETKTYRSNNILRNIDGFKIRPDWP
D8786_RS05870 1 MKKILGVLTILVLLVSVCLYFFTSQPKNIFDEIYQQTEKTYLGNNIFNQLKDVEVHK-YQ
D8786_RS05860 1 MKKILGLIALIALIVLSCFYFFIHQPKNIFDEIYQETEKSYQVDNIFGKNEDIIVRPVWP
D8786_RS05920 1 MKKTLSILAIVIIIISSCFYFFSRQPKNIFDEIYQETEKTYRTNNILRKIDGFEISPGWP
D8786_RS05865 1 MKKILGLVALILLIVLSCFYFFIHQPKNIFDEIYQETEKTYRTNNILRNIEGFEIDDVWP
D8786_RS05885 1 MKKILGLVALFVIIISSCFYFFPKQPKNIFDEIYQETEKTYRSNNILRNIDGFKIRAVWP
D8786_RS05905 1 MKKILGLVALFVIIVLSCFYFFIQQPKNIFDEIYQETEKTYLGNNVFNNLKDVEVHK-YQ
D8786_RS05895 1 MKKILGLVALFVLIILSCFYFFPKQPKNIFDEIYQETEKTYQTNNILRNIEGFDIKPVWP
D8786_RS05910 1 MKKILGLVALVLLVVLFCFYFFPKQPNNIFDEIYQETEKTYHTNNILRNIDGFKIRPDWP
D8786_RS05900 1 MKKILGLVALILLIVLSCFYFFTNHPKNIFDEIYQETEKTYRSNNILRNIDGFKISPGWP
D8786_RS05890 1 MKEILGLVALFVIIISSCFYFFIHQPKNIFDEIYQETEKTYRSNNILRNIEGFEIRPDWP
D8786_RS05940 61 SDDPNISYTPFGKY--ETLPKGYSDITIDLNFGKGIKGVLILFERKTNSNITLWYSAHYN
D8786_RS05930 61 SDDPNISYTPFGKY--ETLTKGYSDITIHFNFGEGIKGVSIRFERKTNSNITLWYSAHYN
D8786_RS05875 61 SDDPNISYTPFGKY--ETLPKGYSDITIDLNFGKGIKGVLILFERKTNSNITLWYSAHYN
D8786_RS05915 61 NDSEYFAYTPSGKY--QTHPEGYKDISIGFNFGSGIKGMTILFEKRINSDITLWYSAHYN
D8786_RS05880 61 NDGEYFAYTPSGKY--QTHPEGYKDISISFNFGEGIKGMTIRFEKRINSDITLWYSAHYN
D8786_RS05870 60 EYDDDSKFYSYVLYQKQKTPHDYKNIDLIFHFTKDTNTVFVXFEKELSNGLRIFIFGRYL
D8786_RS05860 61 SDNESLKYSPHVTY-KDNIFNNYCKVVLGFNFQNLEQTSFIRFDKYIDSGVRIRIRTVYS
D8786_RS05920 61 SDGEYFKYSPLGKY--KTLPEGYLELRVGFNFEKAYSKMFVSVERKIADGTKIWMISKYN
D8786_RS05865 61 SDGDYFKYSPLGKY--KTLPEDYLELRVGFNFEKAYSKMFVSVERKIADGTKLWMVNKYN
D8786_RS05885 61 SDDPNILYTPFGLYNKEKTPSDYSEIEIGFNFQNSQKVLFIYSERRLSSNVSVKVWGSYN
D8786_RS05905 60 EYSDDSKFYPSIVYERNALPDSYEKIAIDFNFKSEAQLSLISFEKLIESNVSIKMWTVYS
D8786_RS05895 61 SDGEFLRYTPSGNY--KNIPEGYLELRIGFSFYSEDEIGSISFEKRIESNVNIKMWTVYS
D8786_RS05910 61 SDDPNILYTPFGLYNKEKTPSDYSEIEIGFNFEYTSQLSSVSFERQVGLNTRVRIWNKYT
D8786_RS05900 61 SDGEYSKYYPFGTYNKDHTPEEYFEVEISFNFATKTQLSSISFEKRIGPNVRVRLWNKYI
D8786_RS05890 61 SDGEYSKYYPFGTYNKDHTPEEYFEIEIGFNFTTKTQLSSISFEKRIGPNVRVRIWDNYT
D8786_RS05940 119 IKKKVLKKELAIFEEPRKPGQFIDDEEKVREYLRKNNISKEELEKDYDEIINQKVLKDWC
D8786_RS05930 119 LQKKVLKKKLAIFEEPRKPGQFIDDEEKVREYLRKNNISKEELEKDFDEIVNQKVLKDWC
D8786_RS05875 119 MQKKVLKKELAIFEEPRKPGQFIDDEEKVREYLRKNNISKEELEKDYDEIINQKVLKDWC
D8786_RS05915 119 IKKKVLQKEIAIFEEPRQPGQYLEDEEKIREYLRKYNISKEELEKDYDEIVNQKVLKDWC
D8786_RS05880 119 MQKKVLKKGLAIFEEPRKPGQYLDDEEKVRNYLKKYNITKEDLEKDYDEIVNQKVLKDWC
D8786_RS05870 120 TKEKLFQKNVQLLINQDGTDKSIEDEAQVKSYLEQYGITAKDLDSYYDEIVNQKVLKDWC
D8786_RS05860 120 YLEKSLKKEVEVIVIKGNSENYIDNESQVKSYLEQYGITAKDLDSYYDEIVNQKVLKDWC
D8786_RS05920 119 PNTKTITKSIQIVL-SGNEDSYIEDEAQVKSYLEKYGITAKDLDSYYDEIVNQKVLKDWC
D8786_RS05865 119 PNTKMITKSIQIVL-SGKEDSYIEDEAQVKSYLEQYGITAKDLDSYYDEIVNQKVLKDWS
D8786_RS05885 121 YKLGVLSKEVTIIKKENNSKVYIDEQSEVKSYLEQYGITTKDLGSYYDDIVNQRVLKDWC
D8786_RS05905 120 HKERSLKKFVKIVLKKAGTKNYIEDEAQVKSYLEQYGITAKDLDSYYDEIVNQKVLKDWC
D8786_RS05895 119 HKERNLKKFVKIGIKKADTETYIEDEAQVKSYLEKYGITAKDLDSYYDEIVNQKVLKDWC
D8786_RS05910 121 YQDRTLKKSVRVVLKKADTETYIEDEAQVKSYLEQYGITAKDLDSYYDEIVNQKVLKDWC
D8786_RS05900 121 RKDRVLKKFVKIGLKKADTETYIEDEAQVKSYLEQYGITAKDLDSYYDEIVNQKVLKDWC
D8786_RS05890 121 RKDRVLKKFVKIGLKKADTETYIEDEAQVKSYLEQYGITAKDLDSYYDEIVNQKVLKDWC
D8786_RS05940 179 TIYDSKYSPSNYGEVKIETQWENW
D8786_RS05930 179 SIYDSKYSPSNYGEVKIETQWENW
D8786_RS05875 179 SIYDSKYSSGNYGEVKVETQWENW
D8786_RS05915 179 SIYDSKYSPSNYGEVKIETQWENW
D8786_RS05880 179 SIYDSKYSPSNYGDVKIETQWENW
D8786_RS05870 180 TIYDSKYSPSNYGDVKVETQWENW
D8786_RS05860 180 SIYDSKYSPSNYGEVKVETQWENW
D8786_RS05920 178 TIYDSKYSPSNYGDVKIETQWENW
D8786_RS05865 178 SIYDSKYSPSNYGDIKIETQWENW
D8786_RS05885 181 SIYDSKYSPSNYGDVKIETQWENW
D8786_RS05905 180 TIYDSKYLPSNYGDVKVETQWENW
D8786_RS05895 179 SIYDSKYSPSNYGEVKVETQWENW
D8786_RS05910 181 TIYDSKYSPSNYGEVKVETQWENW
D8786_RS05900 181 TIYESKYSPSNYGEVKVETQWENW
D8786_RS05890 181 SIYDSKYSPSNYGEVKVETQWENW

Fig 9

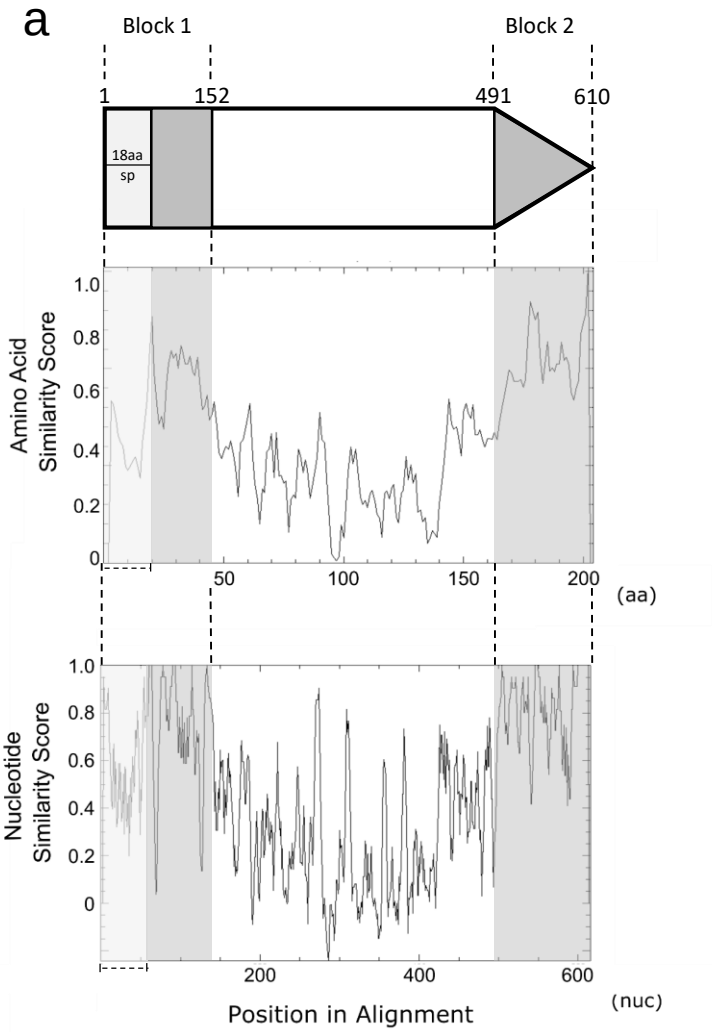
a
Block 1
Block 2
1
152
491
610
18aa
sp
Amino Acid Similarity Score
1.0
0.8
0.6
0.4
0.2
0
50
100
150
200
(aa)
Nucleotide Similarity Score
200
400
600
(nuc)
Position in Alignment

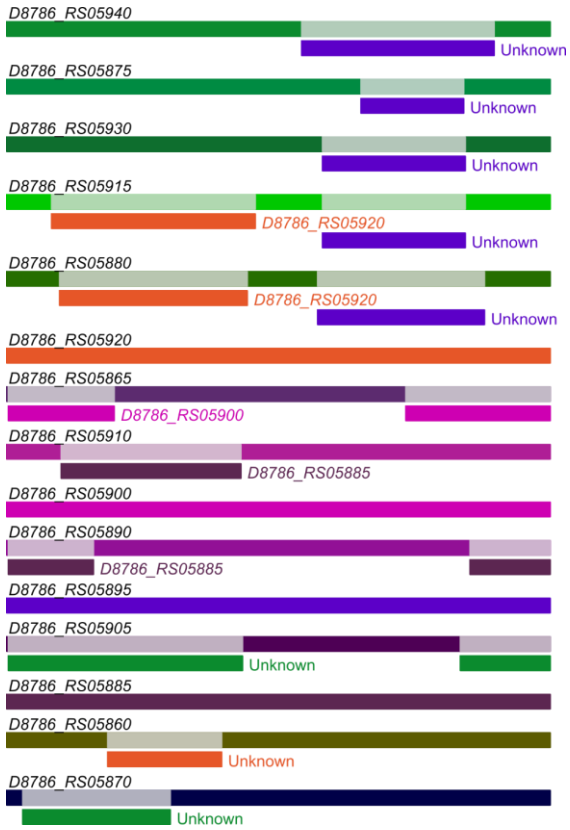
b
D8786_RS05940
Unknown
D8786_RS05875
Unknown
D8786_RS05930
Unknown
D8786_RS05915
D8786_RS05920
Unknown
D8786_RS05880
D8786_RS05920
Unknown
D8786_RS05920
D8786_RS05865
D8786_RS05900
D8786_RS05910
D8786_RS05885
D8786_RS05900
D8786_RS05890
D8786_RS05885
D8786_RS05895
D8786_RS05905
Unknown
D8786_RS05885
D8786_RS05860
Unknown
D8786_RS05870
Unknown

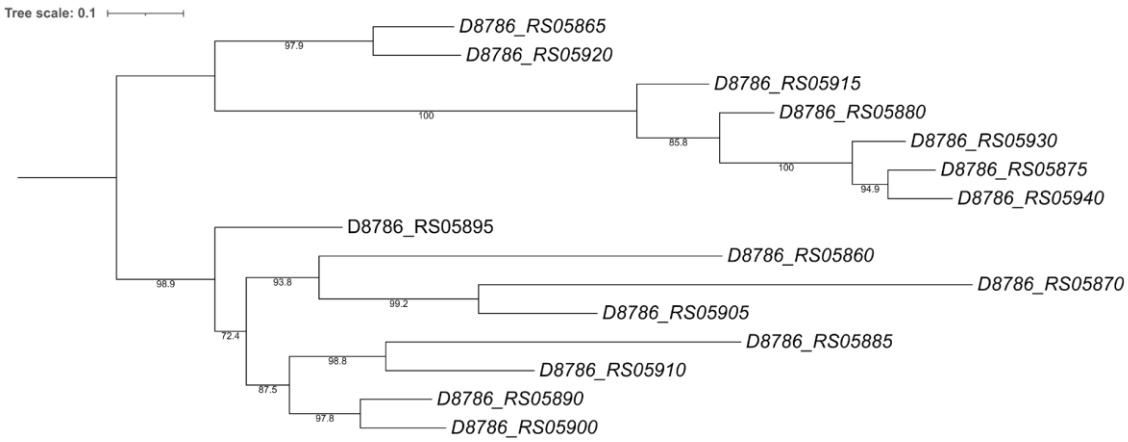
c
Tree scale: 0.1
D8786_RS05865
D8786_RS05920
D8786_RS05915
D8786_RS05880
D8786_RS05930
D8786_RS05875
D8786_RS05940
D8786_RS05895
D8786_RS05860
D8786_RS05870
D8786_RS05905
D8786_RS05885
D8786_RS05910
D8786_RS05890
D8786_RS05900

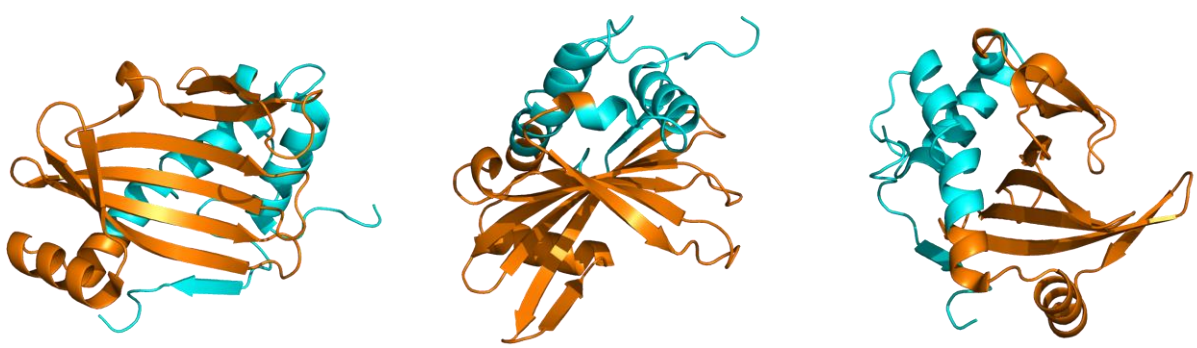
d

Fig 10

a

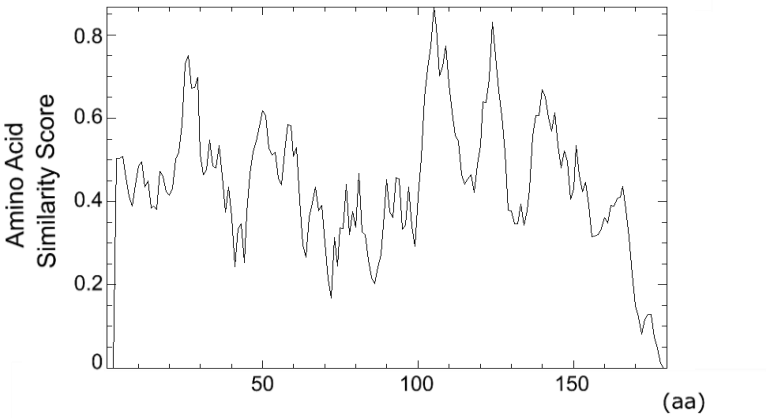
Amino Acid
Similarity Score
0
0.2
0.4
0.6
0.8
50
100
150
(aa)

b

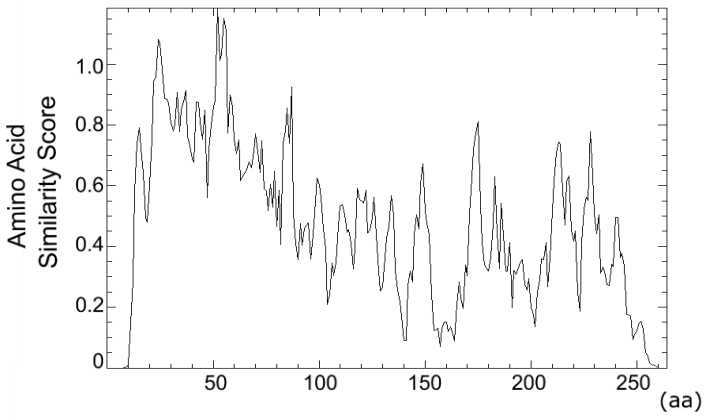
Amino Acid
Similarity Score
0
0.2
0.4
0.6
0.8
1.0
50
100
150
200
250
(aa)

Sup Fig 1

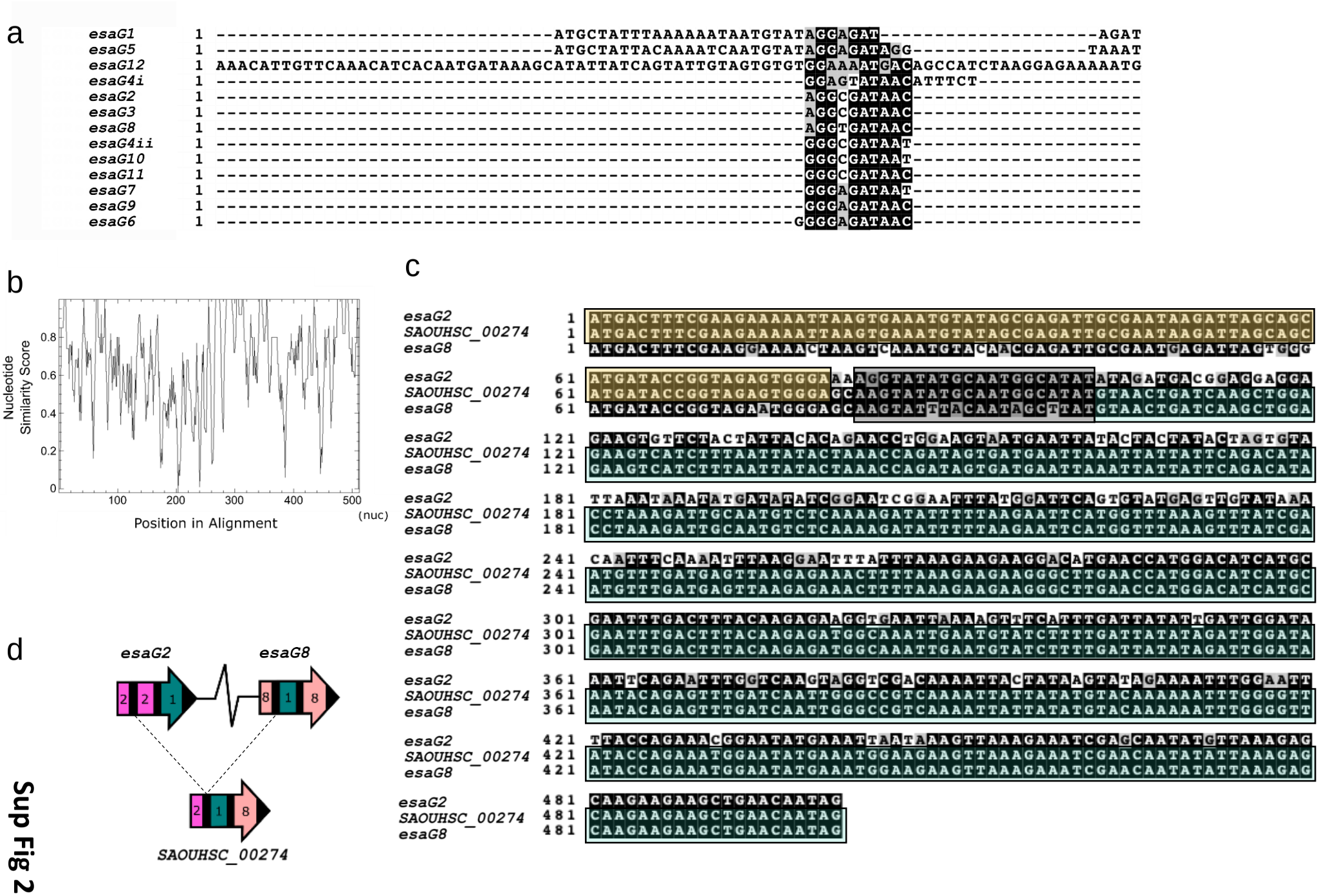
a
esaG1 1 ATGCTATTTAAAAAATAATGTATAGGAGAT AGAT
esaG5 1 ATGCTATTACAAAATCAATGTATAGGAGATAGG TAAAT
esaG12 1 AAACATTGTTCAAACATCACAATGATAAAGCATATTATCAGTATTGTAGTGTGTGGAAAATGACAGCCATCTAAGGAGAAAAATG
esaG4i 1 GGAGTATAACATTTCT
esaG2 1 AGGCGATAAC
esaG3 1 AGGCGATAAC
esaG8 1 AGGTGATAAC
esaG4ii 1 GGGCGATAAT
esaG10 1 GGGCGATAAT
esaG11 1 GGGCGATAAC
esaG7 1 GGGAGATAAT
esaG9 1 GGGAGATAAC
esaG6 1 GGGGAGATAAC
b
Nucleotide Similarity Score
0
0.2
0.4
0.6
0.8
100
200
300
400
500
(nuc)
Position in Alignment
c
esaG2 1 ATGACTTTCGAAGAAAAATTAAGTGAAATGTATAGCGAGATTGCGAATAAGATTAGCAGC
SAOUHSC_00274 1 ATGACTTTCGAAGAAAAATTAAGTGAAATGTATAGCGAGATTGCGAATAAGATTAGCAGC
esaG8 1 ATGACTTTCGAAGGAAAACTAAGTCAAATGTACAACGAGATTGCGAATGAGATTAGTGGG
esaG2 61 ATGATACCGGTAGAGTGGGAAAAGGTATATGCAATGGCATATATAGATGACGGAGGAGGA
SAOUHSC_00274 61 ATGATACCGGTAGAGTGGGAGCAAGTATATGCAATGGCATATGTAACTGATCAAGCTGGA
esaG8 61 ATGATACCGGTAGAATGGGAGCAAGTATTTACAATAGCTTATGTAACTGATCAAGCTGGA
esaG2 121 GAAGTGTTCTACTATTACACAGAACCTGGAAGTAATGAATTATACTACTATACTAGTGTA
SAOUHSC_00274 121 GAAGTCATCTTTAATTATACTAAACCAGATAGTGATGAATTAAATTATTATTCAGACATA
esaG8 121 GAAGTCATCTTTAATTATACTAAACCAGATAGTGATGAATTAAATTATTATTCAGACATA
esaG2 181 TTAAATAAATATGATATATCGGAATCGGAATTTATGGATTCAGTGTATGAGTTGTATAAA
SAOUHSC_00274 181 CCTAAAGATTGCAATGTCTCAAAAGATATTTTTAAGAATTCATGGTTTAAAGTTTATCGA
esaG8 181 CCTAAAGATTGCAATGTCTCAAAAGATATTTTTAAGAATTCATGGTTTAAAGTTTATCGA
esaG2 241 CAATTTCAAAATTTAAGGAATTTATTTAAAGAAGAAGGACATGAACCATGGACATCATGC
SAOUHSC_00274 241 ATGTTTGATGAGTTAAGAGAAACTTTTAAAGAAGAAGGGCTTGAACCATGGACATCATGC
esaG8 241 ATGTTTGATGAGTTAAGAGAAACTTTTAAAGAAGAAGGGCTTGAACCATGGACATCATGC
esaG2 301 GAATTTGACTTTACAAGAGAAGGTGAATTAAAAGTTTCATTTGATTATATTGATTGGATA
SAOUHSC_00274 301 GAATTTGACTTTACAAGAGATGGCAAATTGAATGTATCTTTTGATTATATAGATTGGATA
esaG8 301 GAATTTGACTTTACAAGAGATGGCAAATTGAATGTATCTTTTGATTATATAGATTGGATA
esaG2 361 AATTCAGAATTTGGTCAAGTAGGTCGACAAAATTACTATAAGTATAGAAAATTTGGAATT
SAOUHSC_00274 361 AATACAGAGTTTGATCAATTGGGCCGTCAAAATTATTATATGTACAAAAAATTTGGGGTT
esaG8 361 AATACAGAGTTTGATCAATTGGGCCGTCAAAATTATTATATGTACAAAAAATTTGGGGTT
esaG2 421 TTACCAGAAACGGAATATGAAATTAATAAAGTTAAAGAAATCGAGCAATATGTTAAAGAG
SAOUHSC_00274 421 ATACCAGAAATGGAATATGAAATGGAAGAAGTTAAAGAAATCGAACAATATATTAAAGAG
esaG8 421 ATACCAGAAATGGAATATGAAATGGAAGAAGTTAAAGAAATCGAACAATATATTAAAGAG
esaG2 481 CAAGAAGAAGCTGAACAATAG
SAOUHSC_00274 481 CAAGAAGAAGCTGAACAATAG
esaG8 481 CAAGAAGAAGCTGAACAATAG
d
esaG2
esaG8
2 2 1
8 1 8
2 1 8
SAOUHSC_00274

Sup Fig 2

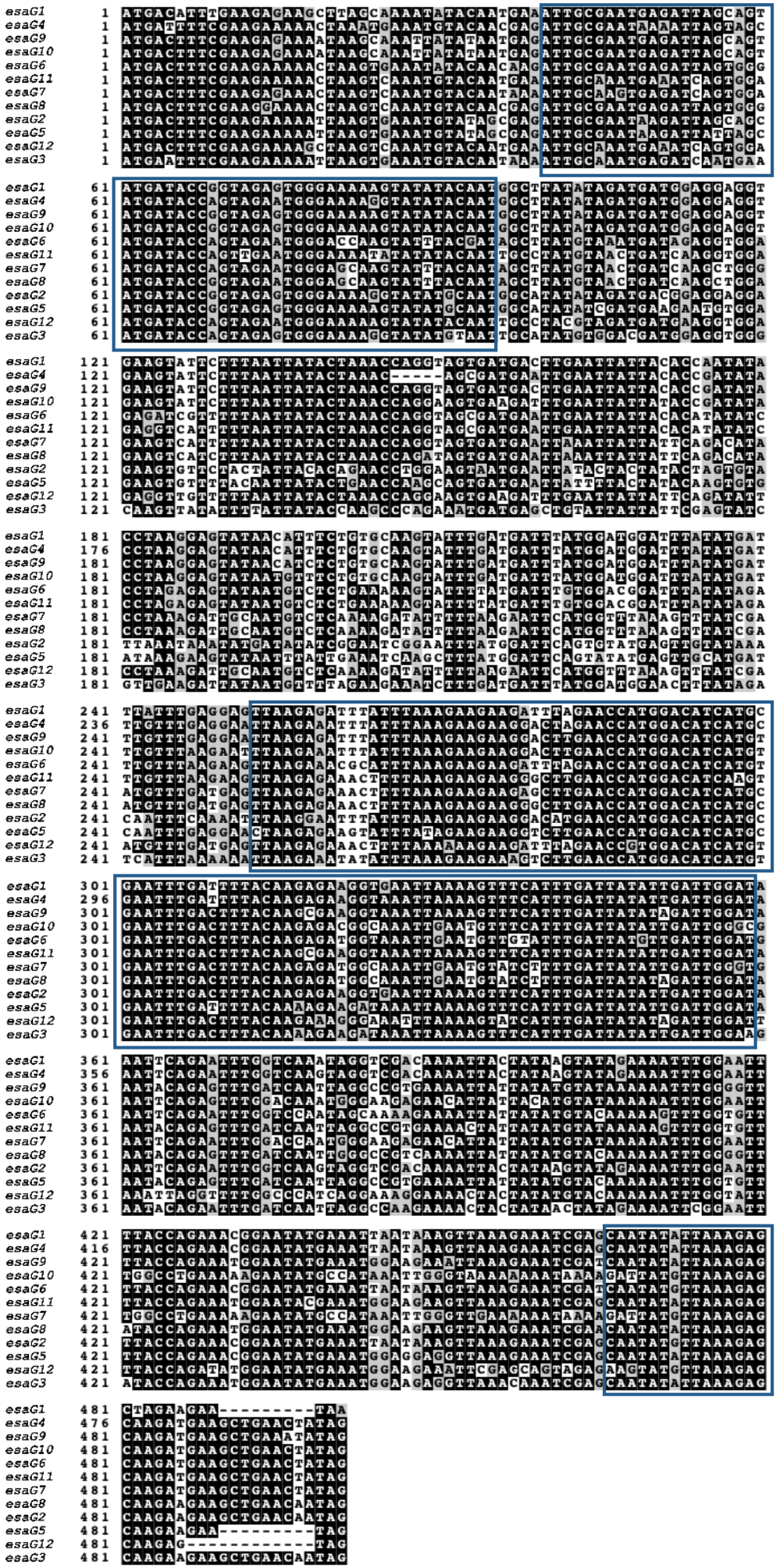
esaG1
esaG4
esaG9
esaG10
esaG6
esaG11
esaG7
esaG8
esaG2
esaG5
esaG12
esaG3

Sup Fig 3

a


esaE
esxD
esaD
esaG
SAUSA300_0290
SAUSA300_0291
SAUSA300_0292
SAUSA300_0293
SAUSA300_0294
SAUSA300_0295
SAUSA300_0296
SAUSA300_0297
SAUSA300_0298
SAUSA300_0299
SAUSA300_0300
SAUSA300_0301
SAUSA300_0302
SAUSA300_0303
USA300 FPR3757
USA300 BKV_2
esaG4
Chaperone protein, EsaE
WXG100-like protein
T7 secreted nuclease, EsaD
SAOUHSC_00270 homologue
Hypothetical protein
Immunity protein, EsaG
Pseudogene

b

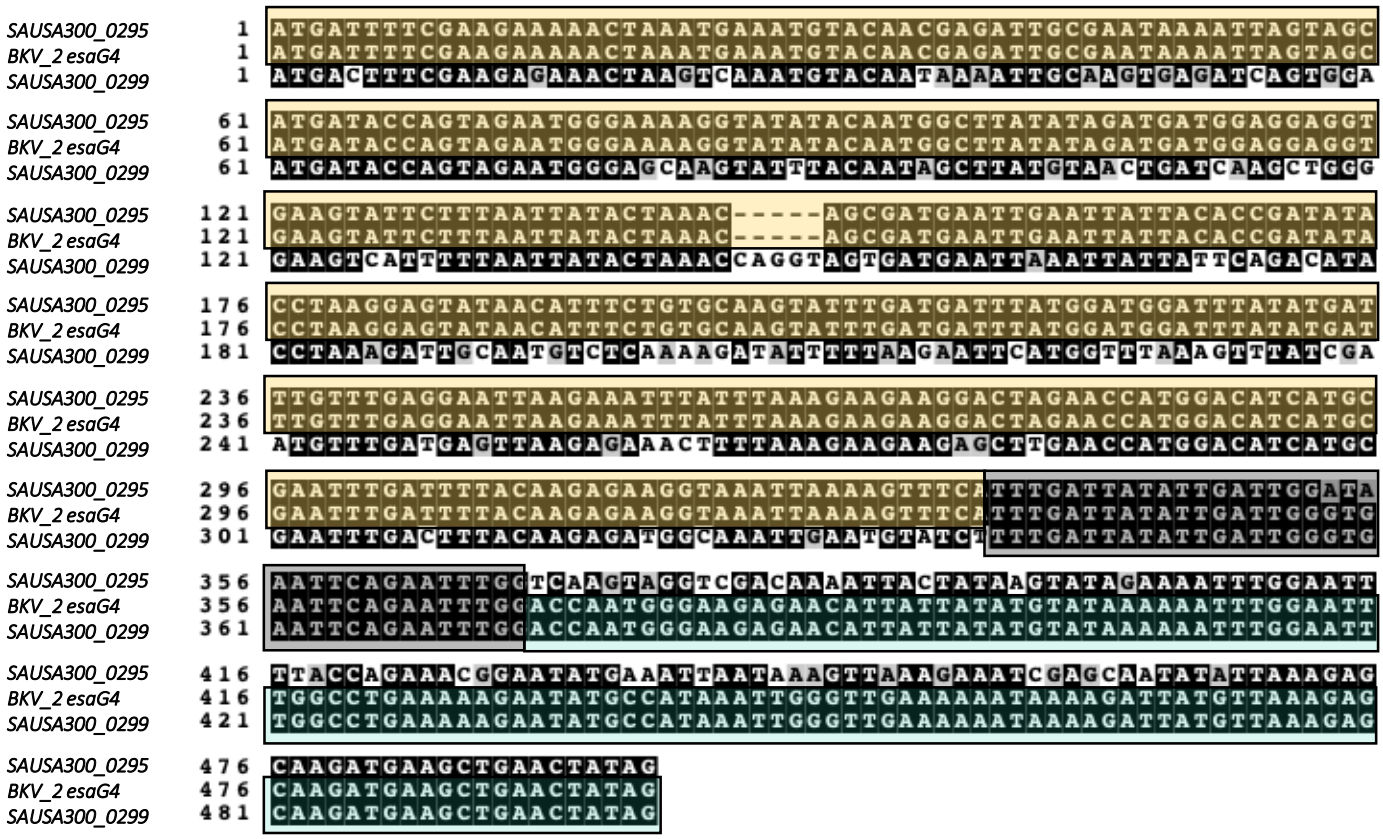
SAUSA300_0295 1 ATGATTTTCGAAGAAAAACTAAATGAAATGTACAACGAGATTGCGAATAAAATTAGTAGC
BKV_2 esaG4 1 ATGATTTTCGAAGAAAAACTAAATGAAATGTACAACGAGATTGCGAATAAAATTAGTAGC
SAUSA300_0299 1 ATGACTTTCGAAGAGAAACTAAGTCAAATGTACAATAAAATTGCAAGTGAGATCAGTGGA
SAUSA300_0295 61 ATGATACCAGTAGAATGGGAAAAGGTATATACAATGGCTTATATAGATGATGGAGGAGGT
BKV_2 esaG4 61 ATGATACCAGTAGAATGGGAAAAGGTATATACAATGGCTTATATAGATGATGGAGGAGGT
SAUSA300_0299 61 ATGATACCAGTAGAATGGGAGCAAGTATTTACAATAGCTTATGTAACTGATCAAGCTGGG
SAUSA300_0295 121 GAAGTATTCTTTAATTATACTAAAC-----AGCGATGAATTGAATTATTACACCGATATA
BKV_2 esaG4 121 GAAGTATTCTTTAATTATACTAAAC-----AGCGATGAATTGAATTATTACACCGATATA
SAUSA300_0299 121 GAAGTCATTTTTAATTATACTAAACCAGGTAGTGATGAATTAAATTATTATTCAGACATA
SAUSA300_0295 176 CCTAAGGAGTATAACATTTCTGTGCAAGTATTTGATGATTTATGGATGGATTTATATGAT
BKV_2 esaG4 176 CCTAAGGAGTATAACATTTCTGTGCAAGTATTTGATGATTTATGGATGGATTTATATGAT
SAUSA300_0299 181 CCTAAAGATTGCAATGTCTCAAAAGATATTTTAAGAATTCATGGTTTAAAGTTTATCGA
SAUSA300_0295 236 TTGTTTGAGGAATTAAGAAATTTATTTAAAGAAGAAGGACTAGAACCATGGACATCATGC
BKV_2 esaG4 236 TTGTTTGAGGAATTAAGAAATTTATTTAAAGAAGAAGGACTAGAACCATGGACATCATGC
SAUSA300_0299 241 ATGTTTGATGAGTTAAGAGAAACTTTAAAGAAGAAGAGCTTGAACCATGGACATCATGC
SAUSA300_0295 296 GAATTTGATTTTACAAGAGAAGGTAAATTAAAAGTTTCATTTGATTATATTGATTGGATA
BKV_2 esaG4 296 GAATTTGATTTTACAAGAGAAGGTAAATTAAAAGTTTCATTTGATTATATTGATTGGGTG
SAUSA300_0299 301 GAATTTGACTTTACAAGAGATGGCAAATTGAATGTATCTTTTGATTATATTGATTGGGTG
SAUSA300_0295 356 AATTCAGAATTTGGTCAAGTAGGTCGACAAAATTACTATAAGTATAGAAAATTTGGAATT
BKV_2 esaG4 356 AATTCAGAATTTGGACCAATGGGAAGAGAACATTATTATATGTATAAAAAATTTGGAATT
SAUSA300_0299 361 AATTCAGAATTTGGACCAATGGGAAGAGAACATTATTATATGTATAAAAAATTTGGAATT
SAUSA300_0295 416 TTACCAGAAACGGAATATGAAATTAATAAAGTTAAAGAAATCGAGCAATATATTAAAGAG
BKV_2 esaG4 416 TGGCCTGAAAAAGAATATGCCATAAATTGGGTTGAAAAAATAAAAGATTATGTTAAAGAG
SAUSA300_0299 421 TGGCCTGAAAAAGAATATGCCATAAATTGGGTTGAAAAAATAAAAGATTATGTTAAAGAG
SAUSA300_0295 476 CAAGATGAAGCTGAACTATAG
BKV_2 esaG4 476 CAAGATGAAGCTGAACTATAG
SAUSA300_0299 481 CAAGATGAAGCTGAACTATAG

Sup Fig 4


a
esaG1
esaG2
esaG4
esaG4
Unknown
esaG10
Unknown
esaG6
SAPIG_0314
esaG11
esaG7
esaG12
esaG8
esaG12
esaG12
esaG11
SAPIG_0314
esaG2
esaG4
SAPIG_0310
esaG4
esaG5
esaG11
SAPIG_0311
SAPIG_0314
esaG3
b
esaG1
esaG2
esaG4
esaG2
esaG9
SAR_0293
esaG10
esaG12
SAR_0294
esaG12
esaG6
esaG11
esaG5
SAR_0295
SAR_0293
esaG3
esaG7
SAR_0294
esaG8
esaG12
esaG2
Unknown
SAR_0293
Unknown
esaG5
esaG3
esaG12
SAR_0296
SAR_0294
c
esaG1
esaG4
Unknown
esaG9
esaG5
esaG10
Unknown
esaG6
esaG11
SAEMRSA15_02570
esaG6
SAEMRSA15_02580
esaG6
SAEMRSA15_02570
esaG1
esaG7
esaG12
esaG8
Unknown
esaG2
esaG4
esaG5
Unknown
esaG12
esaG8
esaG3

Sup Fig 5

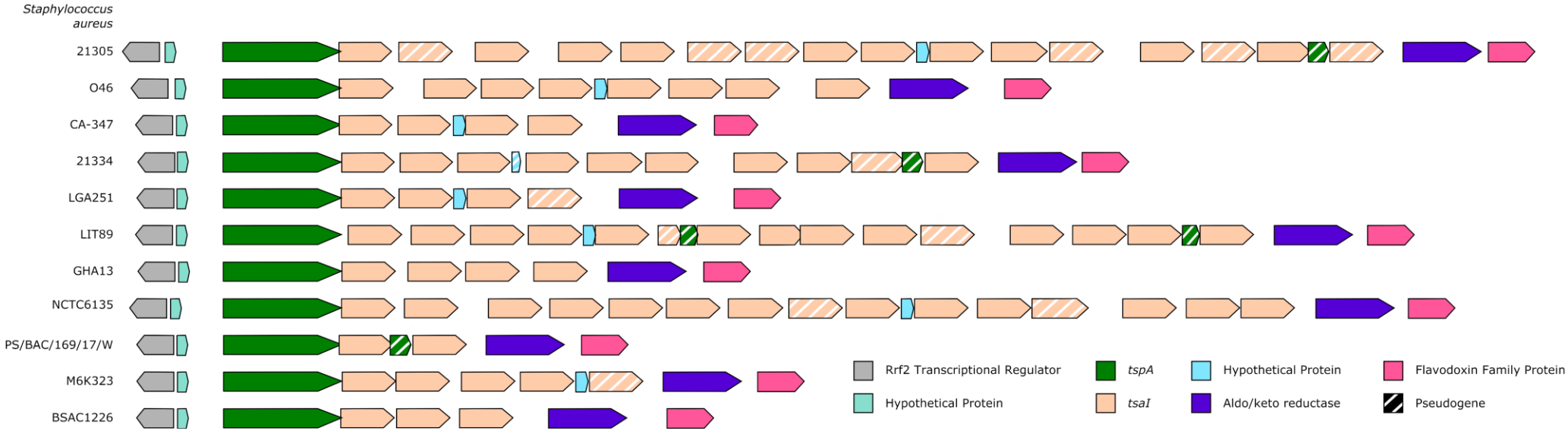
Staphylococcus aureus
21305
O46
CA-347
21334
LGA251
LIT89
GHA13
NCTC6135
PS/BAC/169/17/W
M6K323
BSAC1226
Rrf2 Transcriptional Regulator
Hypothetical Protein
tspA
tsaI
Hypothetical Protein
Aldo/keto reductase
Flavodoxin Family Protein
Pseudogene

Sup Fig 6

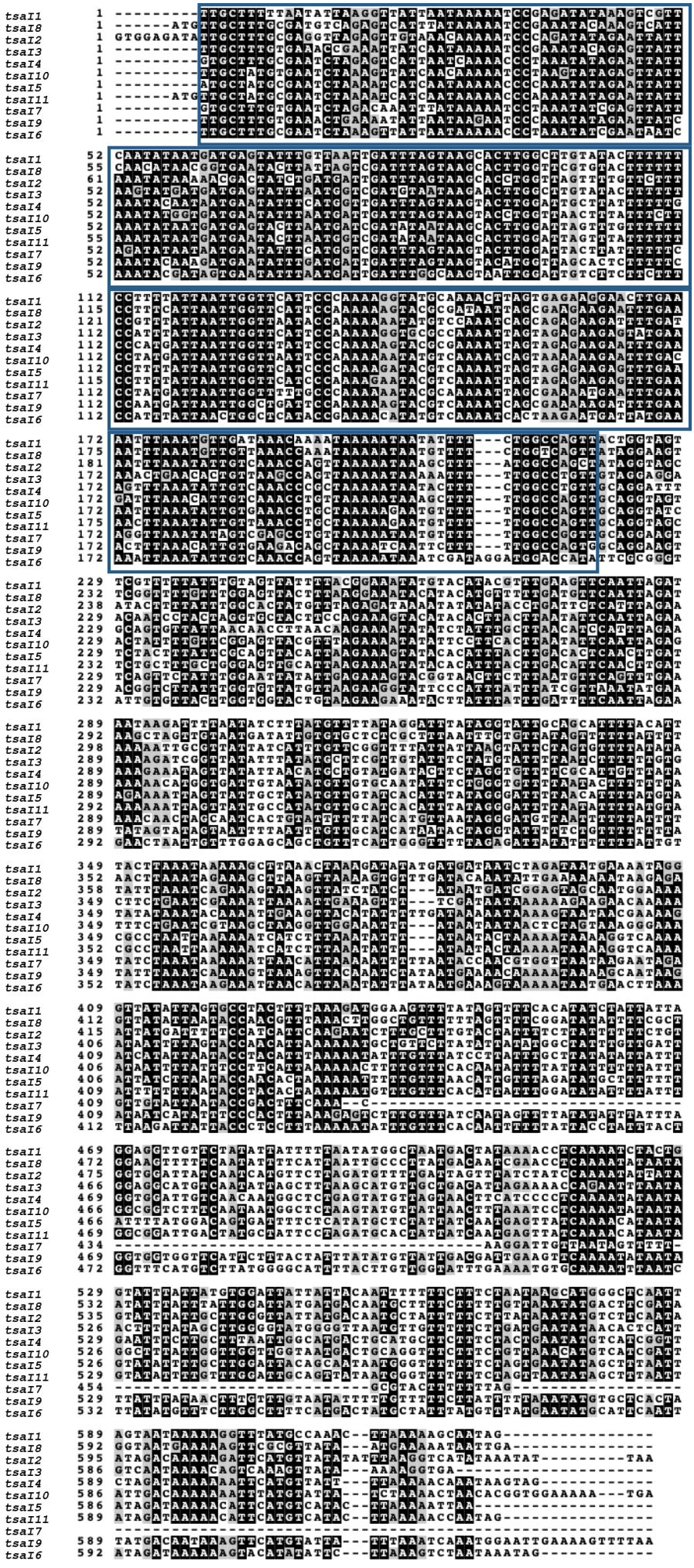
tsaI1
tsaI8
tsaI2
tsaI3
tsaI4
tsaI10
tsaI5
tsaI11
tsaI7
tsaI9
tsaI6

Sup Fig 7

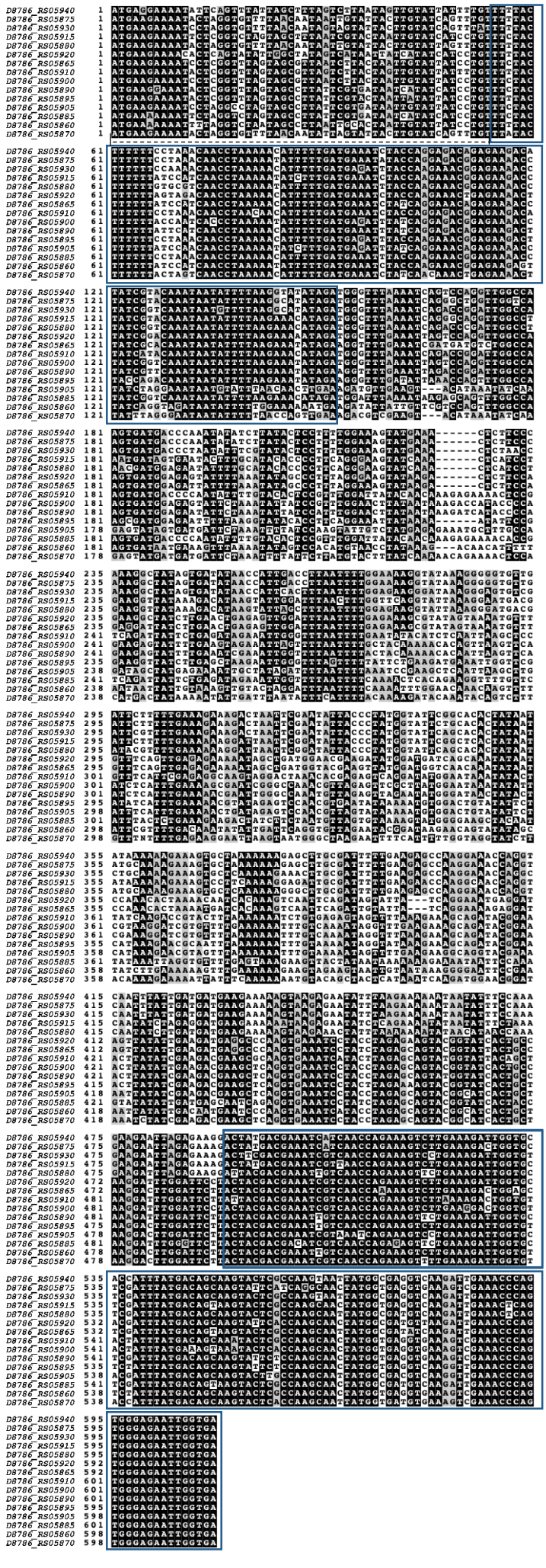
D8786_RS05940
D8786_RS05875
D8786_RS05930
D8786_RS05915
D8786_RS05880
D8786_RS05920
D8786_RS05865
D8786_RS05910
D8786_RS05900
D8786_RS05890
D8786_RS05895
D8786_RS05905
D8786_RS05885
D8786_RS05860
D8786_RS05870

Sup Fig 8